POLITECNICO DI TORINO

Master's degree course in Aerospace Engineering

Master Thesis

Analysis and implementation of Virtual Element Methods for the Stokes Problem

Supervisors
Prof. Stefano Berrone
Prof. Andrea Borio

Candidate
Elisa Naimo

Academic year 2019-2020

Abstract

Stokes equations allow to describe various problems of engineering interest, such as problems of lubrication and sedimentation.

A method to solve these types of problem, which allows to obtain a divergence-free solution for the velocity field consistent with the pressure field, is the Virtual Elements Method (VEM).

First, the theory of VEM and its application to the Stokes problem were investigated. Subsequently, a tool was developed for the implementation of VEM to second order differential problems on polygonal meshes, which can deal with geometrically complex polygons, such as non-convex or high aspect ratio elements.

Contents

List of Figures

List of Tables

Introduction

The Finite Element Method is a numerical method that reduces partial differential equations to a system of algebraic equations, providing an approximate solution to many physical phenomena.

The main feature of the finite element method is the discretization of the domain through the creation of a mesh generated by the repetition of a shape (triangles and quadrilaterals for 2D domains or tetrahedra and hexahedra for 3D domains). On each element characterized by this elementary form, the solution of the problem is assumed to be expressed by a polynomial function. The basis functions generating this polynomial space are named shape functions.

The Virtual Element Method, which has been developed for a large range of mathematical and engineering problems with successfully results, is an extension of the Finite Element Method to general polygonal or polyhedral elements. The interest for polygonal and polyhedral meshes is growing, and their use in commercial codes is increasing. VEM further improve this aspect allowing combination of element with different shape or number of edges in the same mesh.

There are a lot of different approaches to the approximate solution of PDE problems and most of these methods use different trial and test functions. VEM uses trial and test function that are solutions of PDEs inside each element.

The key features of VEM of order k are:

- the trial and test functions contain all polynomials of degree $\leq k$ and a non-polynomial part;
- if one of the two entries of the bilinear form is polynomial the local stiffness matrix is computable in the exact form for the VEM problem since the non-polynomial part is taken as a degree of freedom;
- if both entries are non-polynomials it is only required that the result has the right order of magnitude and some stability properties.

In this thesis we propose a solution to the Stokes Problem in a two-dimensional domain by means of the VEM of order $k = 2$ and $k = 1$.

This approach gives a discretized solution of the pointwise divergence-free velocity vector and of the pressure, which is assumed to be of order $k - 1$ in each element.

This thesis has the following layout: the first chapter describes the Stokes problem, focusing on the variational formulation and the conditions to obtain a stable solution. The second chapter shows, from a theoretical point of view, the Virtual Elements Method for the Stokes problem, giving a definition of the Virtual spaces and the degrees of freedom. The third chapter shows the implementation of the Virtual Elements Method in Matlab, focusing on the evaluation of the projection operators. Chapter four deals with the definition of a reduced formulation of the Stokes problem. Chapter five shows the meshes and the numerical results, along with the computation of the error convergence rate. Finally, chapter six presents some final remarks and possible future work.

Chapter 1

Stokes Problem

1.1 Stokes flow

The Stokes problem models the slow flow of a viscous fluid, the so called *creeping flow*. It is a flow in which inertia is negligible compared to viscous and pressure forces, momentum is transported only by viscous diffusion and not by convection. The formal requirement is to the Reynolds number to be small: $Re \ll 1$.

A highly viscous flow may result in a low Reynolds number. Thus, the Stokes problem describes an object that move within a syrupy fluid or a syrupy fluid that is pumped through a conduit. The forces that are generated by the motion are frictional forces.

A common application of low Reynolds number flow is the study of small suspended particles. The flow around the particles produces local velocity gradients and local energy dissipation. This is the case, for example, of a dusty gas whose particles are very small - whose size range is approximately $10 - 100\ \mu m$. By solving the problem it is possible to determine an effective viscous stress due to the presence of particles.

The Stokes problem is also considered when studying low Reynolds number hydrodynamics, particularly when studying flow in micro-scale devices. Another application, which has to do with both high viscosity and small channels, is hydrodynamic lubrication. Flow through the gaps between bearings and races is governed by a balance between pressure gradient and viscous friction. Pressures in bearing spaces are often extremely high because the oil can prevent surfaces from coming into contact with each other.

1.2 Stokes equations

The equation describing the Stokes flow can be derived from the conservation form of the momentum Navier-Stokes equation.

Considering that the momentum per unit of volume is $\rho\mathbf{u}$, its variation depends on the sum of the momentum flux and of the field forces per unit of volume and per unit of surface area.

$$\frac{d}{dt}\int_\Omega \rho\mathbf{u}\, d\Omega = -\oint_\sigma \rho\mathbf{u}(\mathbf{u}\cdot\mathbf{n})\, d\sigma + \oint_\sigma \mathbf{\Pi}\cdot\mathbf{n}\, d\sigma + \int_\Omega \rho\mathbf{f}\, d\Omega \tag{1.1}$$

where $\mathbf{u}$ is the velocity field of the fluid and ρ the fluid density, $\mathbf{\Pi}$ is the sum of viscous and pressure stresses, and $\mathbf{f}$ is an applied body force. Ω represents a volume, σ is its outer surface and $\mathbf{n}$ is the normal to the surface σ.

Exploiting the divergence theorem, Equation 1.1 can be wrote as:

$$\int_\Omega \frac{\partial}{\partial t}(\rho\mathbf{u})\, d\Omega = -\int_\Omega \text{div}\ (\rho\mathbf{u}\mathbf{u})\, d\Omega + \int_\Omega \text{div}\ (\mathbf{\Pi})\, d\Omega + \int_\Omega \rho\mathbf{f}\, d\Omega$$

To obtain the differential form of the momentum equation:

$$\frac{\partial}{\partial t}(\rho\mathbf{u}) + \text{div}\ (\rho\mathbf{u}\mathbf{u}) = \text{div}\ \mathbf{\Pi} + \rho\mathbf{f} \tag{1.2}$$

Assuming that the fluid is incompressible and that the Reynolds number is very low, the term on the left vanishes and the following represents the momentum equation for the Stokes flow:

$$\text{div}\ \mathbf{\Pi} + \mathbf{f} = 0 \tag{1.3}$$

The divergence of the stress tensor can be expressed as:

$$\text{div}\ \mathbf{\Pi}(\mathbf{u}, p) = -\nabla p + 2\mu\ \text{div}\ \boldsymbol{\varepsilon}(\mathbf{u}) \tag{1.4}$$

where p is the pressure field and μ is the dynamic viscosity. Regarding the operators, ∇ the gradient for scalar functions and div the divergence.

This thesis focuses on the Stokes Problem on a polygonal domain $\Omega \subseteq \mathbb{R}^2$ with homogeneous Dirichlet boundary conditions:

$$\begin{cases} \text{find } (\mathbf{u},p) \text{ such that} & \\ -2\mu\ \text{div}\ \boldsymbol{\varepsilon}(\mathbf{u}) + \nabla p = \mathbf{f} & \text{in } \Omega \\ \text{div}\ \mathbf{u} = 0 & \text{in } \Omega \\ \mathbf{u} = 0 & \text{on } \Gamma = \partial\Omega \end{cases} \tag{1.5}$$

$\boldsymbol{\varepsilon}(\mathbf{u})$ is the linearized strain tensor or the symmetric part of the gradient of $\mathbf{u}$:

$$\boldsymbol{\varepsilon}(\mathbf{u}) = \frac{\nabla\mathbf{u} + \nabla\mathbf{u}^T}{2} \tag{1.6}$$

The mass conservation equation can be written as:

$$\frac{\partial\rho}{\partial t} + \text{div}\ (\rho\mathbf{u}) = 0 \tag{1.7}$$

For an incompressible flow, Equation 1.7 become:

$$\text{div } \mathbf{u} = 0$$

$\mathbf{u}$ is called *divergence-free* or solenoidal.

1.2.1 Boundary conditions

The last condition in Equation 1.5 represents the no-slip condition for the problem.

Physically, the condition $u_n = 0$ models an impermeable wall. In particular, referring to the principle of conservation of mass, no mass is lost or gained across this boundary.

The conditions on the tangential velocity model the fact that the velocity at the wall is zero because of viscosity.

1.3 Variational formulation

In order to simplify the subsequent discussion, it is customary to replace the strain tensor by the gradient.

$$\begin{cases} \text{find } (\mathbf{u},p) \text{ such that} & \\ -\mu\boldsymbol{\Delta}\mathbf{u} + \nabla p = \mathbf{f} & \text{in } \Omega \\ \text{div } \mathbf{u} = 0 & \text{in } \Omega \\ \mathbf{u} = 0 & \text{on } \Gamma = \partial\Omega \end{cases} \tag{1.8}$$

where $\boldsymbol{\Delta}$ denotes the vector Laplacian.

Assuming $\mathbf{u}$ and $\mathbf{v}$ are respectively the trial and test function, the weak form of Equation 1.8 is:

$$\begin{cases} \text{find } (\mathbf{u},p) \text{ such that} & \\ \displaystyle\int_\Omega \mu\boldsymbol{\nabla}\mathbf{u} : \boldsymbol{\nabla}\mathbf{v}\, d\Omega - \int_\Omega p \text{ div } \mathbf{v}\, d\Omega = \int_\Omega \mathbf{f}\cdot\mathbf{v}\, d\Omega & \text{in } \Omega \\ \displaystyle\int_\Omega q \text{ div } \mathbf{u} = 0 & \text{in } \Omega \\ \mathbf{u} = 0 & \text{on } \Gamma = \partial\Omega \end{cases} \tag{1.9}$$

It is easy to prove that the pressure p is determined by the Stokes equations only up to a constant.

For any divergence-free function $\mathbf{u}$, the following relation holds:

$$\int_\Omega \text{div } \mathbf{u}\, dx = \int_{\partial\Omega} \mathbf{u}\cdot\mathbf{n}\, ds = 0$$

The only term the Equation 1.9 which determines the pressure is:

$$\int_\Omega p \text{ div } \mathbf{v}\, dx = -\int_\Omega \mathbf{v}\nabla p\, dx + \int_{\partial\Omega} \mathbf{v}\cdot\mathbf{n}\, p\, ds = -\int_\Omega \mathbf{v}\nabla\mathbf{p}\, dx \tag{1.10}$$

If p_0 is a constant value pressure, its gradient is zero. According to Equation 1.10, it is possible to add any constant p_0 to the solution of p without changing the integral above. Thus, p is determined up to a constant.

1.3.1 Bilinear forms

The trial and test functions $\mathbf{u}$, $\mathbf{v} \in \mathbf{V}$ and the scalar function $q \in Q$. The spaces $\mathbf{V}$ and Q are defined as follows:

$$\mathbf{V} := [H_0^1(\Omega)]^2 \tag{1.11}$$

$$Q := L_0^2(\Omega) = \left\{ q \in L^2(\Omega) \quad s.t. \quad \int_\Omega q\, d\Omega = 0 \right\} \tag{1.12}$$

It is possible to write a variational formulation of the Problem 1.8 using the bilinear forms $a(\cdot,\cdot)$ and $b(\cdot,\cdot)$.
The bilinear form $a(\cdot,\cdot)\colon \mathbf{V}\times\mathbf{V}\to\mathbb{R}$ and $b(\cdot,\cdot)\colon \mathbf{V}\times Q\to\mathbb{R}$ are defined by:

$$a(\mathbf{u},\mathbf{v}) \coloneqq \int_\Omega \mu\boldsymbol{\nabla}\mathbf{u} : \boldsymbol{\nabla}\mathbf{v}\, d\Omega, \qquad \text{for all } \mathbf{u},\mathbf{v}\in\mathbf{V} \tag{1.13}$$

$$b(\mathbf{v},q) \coloneqq \int_\Omega \text{div } \mathbf{v}\; q\; d\Omega \qquad \text{for all } \mathbf{v}\in\mathbf{V}, q\in Q \tag{1.14}$$

$$(\mathbf{f},\mathbf{v}) \coloneqq \int_\Omega \mathbf{f}\cdot\mathbf{v}\; d\Omega \tag{1.15}$$

A variational formulation of the Problem (1.8) is:

$$\begin{cases} \text{find } (\mathbf{u},p)\in\mathbf{V}\times Q \text{ such that} & \\ a(\mathbf{u},\mathbf{v}) + b(\mathbf{v},p) = (\mathbf{f},\mathbf{v}) & \text{for all } \mathbf{v}\in\mathbf{V}, \\ b(\mathbf{u},q) = 0 & \text{for all } q\in Q. \end{cases} \tag{1.16}$$

1.4 Discrete problem

The discrete version of the Problem 1.16 is the following:

$$\begin{cases} \text{find } (\mathbf{u}_h,p_h)\in\mathbf{V}_h\times Q_h \text{ such that} & \\ a(\mathbf{u}_h,\mathbf{v}_h) + b(\mathbf{v}_h,p_h) = (\mathbf{f}_h,\mathbf{v}_h) & \text{for all } \mathbf{v}_h\in\mathbf{V}_h, \\ b(\mathbf{u}_h,q_h) = 0 & \text{for all } q_h\in Q_h. \end{cases} \tag{1.17}$$

$\{\mathbf{V}_h \in \mathbf{V}\}$ and $\{Q_h \in Q\}$ represent two families of finite dimensional subspaces dependent on the discretization parameter h.

The Problem 1.17 admits a unique solution if the following conditions are verified [9, pp. 308–309]:

1. The bilinear form $a(\cdot,\cdot)$ is coercive:

$$\begin{aligned} &\exists \alpha > 0 \text{ such that } a(\mathbf{v}_h, \mathbf{v}_h) \geq \alpha \|\mathbf{v}_h\|_V^2 \qquad \forall \mathbf{v}_h \in \mathbf{Z}_h \\ &\text{where } \mathbf{Z}_h \coloneqq \{\, \mathbf{v}_h \in \mathbf{V}_h : b(\mathbf{v}_h, q_h) = 0 \quad \forall q_h \in Q_h \,\} \end{aligned} \tag{1.18}$$

2. The bilinear form $a(\cdot,\cdot)$ is continue:

$$\exists \gamma > 0 \text{ such that } |a(\mathbf{v}_h, \mathbf{u}_h)| \leq \gamma \|\mathbf{v}_h\|_V \|\mathbf{u}_h\|_V \quad \forall \mathbf{v}_h, \mathbf{u}_h \in \mathbf{V}_h \tag{1.19}$$

3. The bilinear form $b(\cdot,\cdot)$ is continue:

$$\exists \delta > 0 \text{ such that } |b(\mathbf{v}_h, q_h)| \leq \delta \|\mathbf{v}_h\|_V \|q_h\|_Q \quad \forall \mathbf{v}_h \in \mathbf{V}_h, q_h \in Q_h \tag{1.20}$$

4. Exist $\beta > 0$ such that:

$$\forall q_h \in Q_h, \exists \mathbf{v}_h \in \mathbf{V}_h \colon b(\mathbf{v}_h, q_h) \geq \beta \|\mathbf{v}_h\|_{\mathbf{H}^1(\Omega)} \|q_h\|_{L^2(\Omega)} \tag{1.21}$$

Equation 1.21 can be written as follows:

$$\inf_{q_h \in Q_h, q_h \neq 0} \sup_{\mathbf{v}_h \in \mathbf{V}_h, \mathbf{v}_h \neq 0} \frac{b(\mathbf{v}_h, q_h)}{\|\mathbf{v}_h\|_{\mathbf{H}^1(\Omega)} \|q_h\|_{L^2(\Omega)}} \geq \beta \tag{1.22}$$

Condition 1.22 is known as the inf-sup condition. There are two strategies generally followed to obtain stable elements, called compatible elements:

- to choose the spaces $\mathbf{V}_h$ and Q_h so that the inf-sup condition is verified;
- to stabilize the problem, eliminating spurious modes.

Only methods that satisfy the inf-sup condition have been considered in this discussion.

In the next chapters, the Virtual Elements Method will be investigated and a solution of the Stokes problem will be proposed. In particular, it will be provided a definition of the virtual element spaces $\mathbf{V}_h$ and Q_h which allows to verify the inf-sup condition.

Chapter 2

Virtual Element Method

The Virtual Element Method is an extension of the Finite Element Method to general polygonal or polyhedral meshes. The virtual elements spaces are such as the usual spaces of the finite elements with the addition of suitable non-polynomial functions. The spaces and degrees of freedom are chosen in such a way that the elementary stiffness matrix can be calculated without actually having to calculate these non-polynomial functions, but using only the degrees of freedom.

In this way it is possible to manage without difficulty complicated element geometries, higher order continuity conditions (such as C_1, C_2, ...) or mixed problems. This method is very general and could be applied to a large number of different problems.

2.1 Decomposition of the domain

$\mathcal{T}_h$ is a decomposition of a domain Ω into a finite number of simple polygons E. h_E is the diameter of each element E and h denote the maximum diameter of the elements of $\mathcal{T}_h$.

$$h_E \coloneqq \text{diameter}(E), \qquad h \coloneqq \sup_{E \in \mathcal{T}_h} h_E$$

Each element E in $\mathcal{T}_h$ has to fulfil some assumptions:

A1.1 $\forall h \; \exists \gamma > 0$ such that E is star-shaped with respect to a ball of radius $\geq \gamma h_E$

A1.2 $\forall h \; \exists \gamma > 0$ such that the distance between any two vertexes of E is $\geq \gamma h_E$ or that the lenght of all edges is comparable with its diameter h_E.

2.2 Finite dimensional subspaces

The VEM approximation of the Problem 1.17 is:

$$\begin{cases} \text{find } (\mathbf{u}_h, p_h) \in \mathbf{V}_h \times Q_h \text{ such that} \\ a_h(\mathbf{u}_h, \mathbf{v}_h) + b(\mathbf{v}_h, p_h) = (\mathbf{f}_h, \mathbf{v}_h) & \text{for all } \mathbf{v}_h \in \mathbf{V}_h, \\ b(\mathbf{u}_h, q_h) = 0 & \text{for all } q_h \in Q_h. \end{cases} \tag{2.1}$$

where $\mathbf{V}_h \subset \mathbf{V}$ is the space of discrete velocities, $Q_h \subset Q$ is the space of discrete pressures, $a_h(\mathbf{u}_h, \mathbf{v}_h)$ and $(\mathbf{f}_h, \mathbf{v}_h)$ are the approximation of the following integrals:

$$a_h(\mathbf{u}_h, \mathbf{v}_h) \simeq \nu \int_\Omega \nabla \mathbf{u}_h : \nabla \mathbf{v}_h \qquad \forall \mathbf{v}_h, \mathbf{w}_h \in \mathbf{V}_h$$

$$(\mathbf{f}_h, \mathbf{v}_h) \simeq \int_\Omega \mathbf{f} \cdot \mathbf{v}_h \qquad \forall \mathbf{v}_h \in \mathbf{V}_h.$$

The continuous solution has to verify div $\mathbf{u} = 0$ (Equation 1.16):

$$\mathbf{u} \in \mathbf{Z} = \{\, \mathbf{v} \in \mathbf{V} \text{ s. t. } \operatorname{div} \mathbf{v} = 0 \,\}.$$

Similarly, the discrete solution satisfies the second row of the discrete Problem 2.1:

$$\int_\Omega q_h \operatorname{div} \mathbf{u}_h = 0 \qquad \forall q_h \in Q_h$$

therefore

$$\mathbf{u}_h \in \mathbf{Z}_h = \left\{ \mathbf{v}_h \in \mathbf{V}_h \text{ s. t. } \int_\Omega q_h \operatorname{div} \mathbf{v}_h = 0 \qquad \forall q_h \in Q_h \right\}.$$

Even assuming that the original space $\mathbf{V}_h$ has good approximation properties, it is not guaranteed that $\mathbf{Z}_h$ is sufficiently rich to approximate the solution $\mathbf{u} \in \mathbf{Z}$.

For any finite element formulation, if it exists $\beta > 0$, uniform with respect to h, such that the inf-sup condition is verified (Equation 1.22), it can be showed that the spaces $\mathbf{Z}_h$ and the spaces $\mathbf{V}_h$ approximates $\mathbf{u}$ at the same convergence rate.

For the virtual element formulation, the virtual spaces are defined as follow:

$$Q_h = \left\{ q \in L^2_0(\Omega) : q|_E \in Q_h^E \qquad \forall E \in \mathcal{T}_h \right\} \tag{2.2}$$

$$\mathbf{V}_h = \left\{ \mathbf{v} \in [H^1_0(\Omega)]^2 : \mathbf{v}|_E \in \mathbf{V}_h^E \qquad \forall E \in \mathcal{T}_h \right\} \tag{2.3}$$

The spaces $\mathbf{V}_h$ and Q_h will be defined element-wise by introducing the local spaces $\mathbf{V}_h^E$ and Q_H^E and the associated local degree of freedom.

As regards the local space for velocities, it is defined as follows:

$$\mathbf{V}_h^E := \Bigg\{ \mathbf{v} \in [H^1(E)]^2 \quad \text{s.t.} \quad \mathbf{v}|_{\partial E} \in [\mathbb{B}_k(\partial E)]^2, \\ \begin{cases} -\nu \boldsymbol{\Delta} \mathbf{v} - \nabla s \in \mathcal{G}_{k-2}(E)^\perp, \\ \operatorname{div} \mathbf{v} \in \mathbb{P}_{k-1}(E), \end{cases} \quad \text{for some } s \in L^2(E) \Bigg\} \tag{2.4}$$

VEM functions restricted to the edge ∂E are defined on the space $\mathbb{B}_k(\partial E)$, which is the space of the continuous functions that are polynomials on each edge and $k \in \mathbb{N}$ is the highest degree of the set of polynomials:

$$\mathbb{B}_k(\partial E) \coloneqq \Big\{ v \in C^0(\partial E) \quad s.t. \quad v|_E \in \mathbb{P}_k(e) \quad \forall \text{ edge } e \subset \partial E \Big\}$$

The space $\mathcal{G}_k(E)^\perp$ includes all the vector polynomials $\subseteq [\mathbb{P}_k(E)]^2$ that cannot be written as gradients of a vector polynomial of degree $k+1$:

$$\mathcal{G}_k(E) \coloneqq \nabla \left(\mathbb{P}_{k+1}(E) \right) \subseteq [\mathbb{P}_k(E)]^2$$

and $\mathbb{P}_k(E)$ is the union of two spaces:

$$\mathbb{P}_k(E) = \mathcal{G}_k(E) \oplus \mathcal{G}_k(E)^\perp$$

Inside each polygon E, functions of $\mathbf{V}_h^E$ are solutions to the momentum equation with polynomial data and, in particular, the divergence of a function in $\mathbf{V}_h^E$ is a polynomial of degree $k-1$.

$$\dim(\mathbf{V}_h^E) = 2n_E k + \frac{(k-1)(k-2)}{2} + \frac{(k+1)k}{2} - 1 = 2n_E k + k(k-1) \tag{2.5}$$

For the local space Q_h^E it holds:

$$Q_h^E \coloneqq \mathbb{P}_{k-1}(E) \tag{2.6}$$

and its dimension is:

$$\dim(Q_h^E) = \dim(\mathbb{P}_{k-1}(E)) = \frac{(k+1)k}{2} \tag{2.7}$$

2.3 Degree of freedom

A suitable set of degrees of freedom for the local velocity $\mathbf{v} \in \mathbf{V}_h^E$ can be introduced:

$\mathbf{D}_V 1$: vertex values of $\mathbf{v}$

$\mathbf{D}_V 2$: $k-1$ pointwise values of $\mathbf{v}$ for every edge $e \in \partial E$

$\mathbf{D}_V 3$: the moments:

$$\int_K \mathbf{v} \cdot \mathbf{g}_{k-2}^\perp \, dE \qquad \forall \mathbf{g}_{k-2}^\perp \in \mathcal{G}_{k-2}(E)^\perp$$

$\mathbf{D}_V 4$: the "divergence" moments:

$$\int_E (\text{div } \mathbf{v}) q_{k-1} \, dE \qquad \forall q_{k-1} \in \mathbb{P}_{k-1}(E)/\mathbb{R}$$

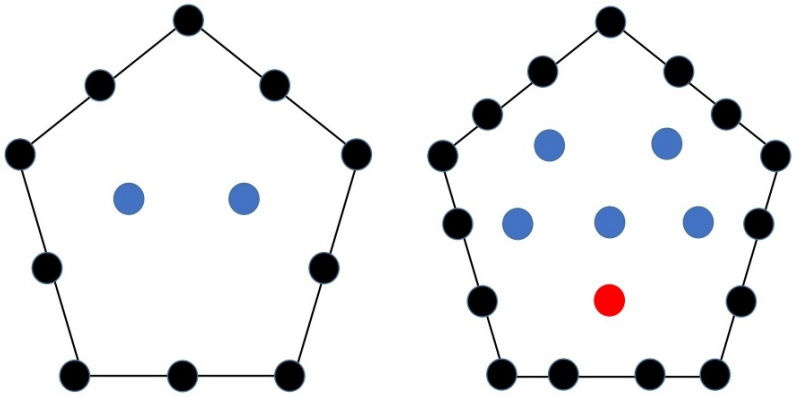

(a) $k = 2$ (b) $k = 3$

Figure 2.1: Degrees of freedom for the local approximation velocity field

In Figure 2.1 there is an idealized depiction of the degrees of freedom $\mathbf{D}_V1$-$\mathbf{D}_V4$. $\mathbf{D}_V1$ and $\mathbf{D}_V2$ are the $2kn_E$ black dots, which are the pointwise degrees of freedom located on the boundary; on the other hand $\mathbf{D}_V4$ are the blue dots and $\mathbf{D}_V3$ are the red dots, which are non-local and are instead defined as a surface integral.

For the local pressure $q \in Q_h^E$:

$\mathbf{D}_Q$: the moments of q:

$$\int_E q p_{k-1}\, dE \qquad \forall p_{k-1} \in \mathbb{P}_{k-1}(E)$$

2.4 Discrete bilinear forms and projection operator

It is now possible to define the discrete bilinear forms of the Problem 2.1. As regards the first bilinear form $a^E(\mathbf{v}, \mathbf{w})$, it can be proved that it is not computable for $(\mathbf{v}, \mathbf{w}) \in \mathbf{V}_h^E \times \mathbf{V}_h^E$. As usually in VEM, it is introduced a computable discrete approximation of the continuous bilinear form $a^E(\cdot, \cdot)$:

$$a_h^E(\cdot, \cdot) : \mathbf{V}_h^E \times \mathbf{V}_h^E \to \mathbb{R} \tag{2.8}$$

with the following properties:

A2.1 k-consistency: for all $\mathbf{q} \in [\mathbb{P}_k(E)]^2$ and $\mathbf{v}_h \in \mathbf{V}_h^E$

$$a_h^E(\mathbf{q}, \mathbf{v}_h) = a^E(\mathbf{q}, \mathbf{v}_h);$$

A2.2 stability: there exist two positive constants α_* and α^*, independent of h and E, such that, for all $\mathbf{v}_h \in \mathbf{V}_h^K$, it holds:

$$\alpha_* a^E(\mathbf{v}_h, \mathbf{v}_h) \leq a_h^E(\mathbf{v}_h, \mathbf{v}_h) \leq \alpha^* a^E(\mathbf{v}_h, \mathbf{v}_h).$$

In order to write a computable form for $a_h^E(\cdot,\cdot)$, it is introduced a projection operator $\Pi_k^{\nabla,E} : \mathbf{V}_h^E \to [\mathbb{P}_k(E)]^2$, for all $E \in \mathcal{T}_h$, defined by:

$$\begin{cases} a^E(\mathbf{q}_k, \mathbf{v}_h - \Pi_k^{\nabla,E}\mathbf{v}_h) = 0 \quad \text{for all } \mathbf{q}_k \in [\mathbb{P}_k(K)]^2, \\ P^{0,E}(\mathbf{v}_h - \Pi_k^{\nabla,K}\mathbf{v}_h) = 0 \end{cases} \tag{2.9}$$

where $P^{0,E}$, defined on E, is the L^2-projection operator onto the constant functions.

The projector operator $\Pi_k^{\nabla,E}$ is computable because the bilinear form $a^E(\mathbf{q}_k, \mathbf{v}_h)$ is computable from the degrees of freedom.

It holds:

$$\Pi_k^{\nabla,E}\mathbf{q}_k = \mathbf{q}_k \qquad \text{for all } \mathbf{q}_h \in \mathbb{P}_k(E) \tag{2.10}$$

Then, writing $a_h^E(\mathbf{u}, \mathbf{v}) = a^E\left(\Pi_k^{\nabla,E}\mathbf{u}_h, \Pi_k^{\nabla,E}\mathbf{v}_h\right)$ will ensure property **A2.1**. Summing a stabilizing term, both **A2.1** and **A2.2** will be verified.

$\mathcal{S}^E(\cdot,\cdot)$ is chosen between the symmetric positive definite bilinear form so that $\mathcal{S}^E(\mathbf{v}, \mathbf{v})$ scales as $a^E(\mathbf{v}, \mathbf{v})$ and it is defined as follows:

$$\begin{aligned} &\exists\, c_0, c_1, \text{ for all } E \text{ and } h_E, \text{ s.t.} \\ &c_0 a^E(\mathbf{v}, \mathbf{v}) \leq \mathcal{S}^E(\mathbf{v}, \mathbf{v}) \leq c_1 a^E(\mathbf{v}, \mathbf{v}) \qquad \forall \mathbf{v} \in \mathbf{V}^E \text{ with } \Pi_k^{\nabla,E}\mathbf{v} = 0 \end{aligned}$$

Then:

$$a_h^E(\mathbf{u}_h, \mathbf{v}_h) \coloneqq a^E\left(\Pi_k^{\nabla,E}\mathbf{u}_h, \Pi_k^{\nabla,E}\mathbf{v}_h\right) + \mathcal{S}^E\left((I - \Pi_k^{\nabla,E})\mathbf{u}_h, (I - \Pi_k^{\nabla,E})\mathbf{v}_h\right) \tag{2.11}$$

The global approximated bilinear form $a_h(\cdot,\cdot) : \mathbf{V}_h \times \mathbf{V}_h \to \mathbb{R}$:

$$a_h(\mathbf{u}_h, \mathbf{v}_h) \coloneqq \sum_{E \in \mathcal{T}_h} a_h^E(\mathbf{u}_h, \mathbf{v}_h) \qquad \text{for all } \mathbf{u}_h, \mathbf{v}_h \in \mathbf{V}_h. \tag{2.12}$$

Regarding $b(\cdot,\cdot)$, it does not require an approximation because it is computable.

$$b(\mathbf{v}_h, q_h) = \sum_{E \in \mathcal{T}_h} b^E(\mathbf{v}_h, q_h) = \sum_{E \in \mathcal{T}_h} \int_E \text{div } \mathbf{v}_h \, q_h \, dE \qquad \text{for all } \mathbf{v}_h \in \mathbf{V}_h, q_h \in Q_h \tag{2.13}$$

2.5 Construction of the right-hand side

Considering the case $k = 2$, $\mathbf{f}_h$ is defined on each element E as the $L^2(E)$-projection of $\mathbf{f}$ onto the space $\mathbb{P}_k$:

$$\Pi_k^{0,E} := [L^2(E)]^2 \to [\mathbb{P}_k(E)]^2]$$

$$\mathbf{f}_h \coloneqq \Pi_k^{0,E}\mathbf{f} \tag{2.14}$$

Thus, the associated righ-hand side is:

$$(\mathbf{f}_h, \mathbf{v}_h) = \sum_{E\in\mathcal{T}_h} \int_E \mathbf{f}_h \cdot \mathbf{v}_h \, dE = \sum_{E\in\mathcal{T}_h} \int_E \Pi_k^{0,E}\mathbf{f} \cdot \mathbf{v}_h \, dE = \sum_{E\in\mathcal{T}_h} \int_E \mathbf{f} \cdot \Pi_k^{0,E}\mathbf{v}_h \, dE \tag{2.15}$$

Chapter 3

Implementation in Matlab

A solution for the Stokes problem has been implemented in Matlab. This Matlab script provides a solution starting from the mesh and from the definition of the reference velocity and pressure fields. The code structure has a main file that calls all the necessary functions. Inside the main file there are the necessary pressure and velocity initializations as symbolic functions, from which the forcing function is easily obtained on the whole reference domain, then the mesh is imported and two structures are created: in the first structure there are all the values related to the degrees of freedom and the number of contributions necessary for the construction of the stiffness matrix, while in the second structure there are all the auxiliary values to the VEM formulation.

After the initializations, there is a for loop which evaluates for each element the local stiffness matrix and the local right-hand side vector.

At the end of the for loop the overall stiffness matrix is built, the system solved and the errors evaluated. The Stokes problem has been solved for three different cases: $k = 1$, $k = 2$ and $k = 2$ with a reduced number of degrees of freedom, as shown in Chapter 4.

3.1 VEM basis

This section describes how the problem is set up to be solved with the VEM, what choices have been made and what kind of functions has been chosen for the discretization. First of all, it is necessary to choose some tools useful to deal with the VEM. One of them is given by the so called scaled-monomial $m_{\boldsymbol{\alpha}}$.

$\{m_{\boldsymbol{\alpha}}^E\}$ is an orthonormal basis in $L^2(E)$ of $\mathbb{P}_k(E)$ defined as follows:

$$m_{\boldsymbol{\alpha}}^E \coloneqq \left(\frac{x - x_E}{h_E}\right)^{\alpha_1} \left(\frac{y - y_E}{h_E}\right)^{\alpha_2} \tag{3.1}$$

where (x_E, y_E) are the coordinates of the centroid of E and h_E its diameter.

As regards $\boldsymbol{\alpha}$, there are the following terms:

$$\boldsymbol{\alpha} := (\alpha_1, \alpha_2) \qquad |\boldsymbol{\alpha}| = \alpha_1 + \alpha_2$$

and:

$$|\boldsymbol{\alpha}| = 0, ..., k$$

It is necessary to vectorize these basis and consider the multi-index $\boldsymbol{\alpha}$ for the two monomials, in such a way as to decouple the equations necessary for the evaluation of the x and y component of the velocity. All the $\boldsymbol{\alpha}$ pairs have been saved and they are summarized in this table:

Table 3.1: Monomial exponent for $k = 2$

i	1	2	3	4	5	6
$\boldsymbol{\alpha}$	(0,0)	(1,0)	(0,1)	(2,0)	(1,1)	(0,2)
k	0	1		2		

Table 3.2: Monomial exponent for $k = 1$

i	1	2	3
$\boldsymbol{\alpha}$	(0,0)	(1,0)	(0,1)
k	0	1	

Basis functions can be represented with the following notation, the first half of the basis is constructed with the second term null and the second half with the first term null:

$$\left\{ \begin{pmatrix} m_i \\ 0 \end{pmatrix} \right\}_{i=1}^{\frac{(k+1)(k+2)}{2}}, \left\{ \begin{pmatrix} 0 \\ m_i \end{pmatrix} \right\}_{i=1}^{\frac{(k+1)(k+2)}{2}}$$

3.1.1 Vandermonde matrices

From the Table 3.1 and 3.2 it is possible to evaluate, for each element, the Vandermonde matrix of order k which has the purpose of containing all the values of the monomial basis in the quadrature points. For this purpose, internal and boundary quadrature points are defined.

To obtain an exact evaluation of the integral it is important that internal quadrature points are in an adequate number with respect to the order of the monomial basis, while on the edge it has been chosen to make the quadrature nodes coincide with the degrees of freedom on the boundary of E in order to guarantee the accuracy of the integral.

It is easy to verify that the first two sets of degrees of freedom ($\mathbf{D}_V1$ and $\mathbf{D}_V2$) allow to obtain the value of the function in the $k+1$ Gauss-Lobatto quadrature nodes, allowing to exactly integrate polynomials on the edges up to order $2k-1$.

Therefore, for each element, the quadrature points are written as $\mathcal{Q}(E)$ and the respective weights $\mathcal{W}(E)$. The Vandermonde matrix of order k is the following [4]:

$$(\mathbf{V}_k^E)_{ij} = m_j(x_i^E), \quad i \in \{1, \dots, N_\mathcal{Q}^E, \quad j \in \{1, \dots, N_k\} \tag{3.2}$$

And the diagonal quadrature weights matrix is defined as:

$$(\mathbf{W}^E)_{ij} = (w^E)_i \delta_{ij} \qquad \forall i, j \in \{1, \dots, N_\mathcal{Q}^E\} \tag{3.3}$$

Where $N_\mathcal{Q}^E$ represents the number of internal quadrature points for the element E and N_k is the number of monomial basis to represents function in a polynomial functions space of order k.

The Vandermonde matrices for the Gauss-Lobatto quadrature points on the edges are indicated in the same way, with the difference that, in this case, the number of points is equal to the number of degrees of freedom on the element edges $N_\mathcal{Q}^{\partial E} = 2kn_E$.

$$(\mathbf{V}_k^{\partial E})_{ij} = m_j(x_i^E), \quad i \in \{1, \dots, N_\mathcal{Q}^{\partial E}, \quad j \in \{1, \dots, N_k\} \tag{3.4}$$

$$(\mathbf{W}^{\partial E})_{ij} = (w^{\partial E})_i \delta_{ij} \qquad \forall i, j \in \{1, \dots, N_\mathcal{Q}^{\partial E}\} \tag{3.5}$$

It is useful for the discussion to consider also the Vandermonde matrices of the derivatives. To do this, the derivative of each monomial base has been evaluated and written as a function of some coefficients for other monomials. All the coefficients are collected in two matrices ($\mathbf{D}_{k,x}$ and $\mathbf{D}_{k,y}$) and these should be multiplied by the Vandermonde matrix.

$$\mathbf{V}_{k,x}^E = \mathbf{V}_k^E \mathbf{D}_{k,x}^E \tag{3.6}$$

$$\mathbf{V}_{k,y}^E = \mathbf{V}_k^E \mathbf{D}_{k,y}^E \tag{3.7}$$

$$\frac{\partial m_j}{\partial x} = \frac{\alpha_1^{(i)}}{h_E} m_i = \sum_{i=1}^{N_k} (\mathbf{D}_{k,x}^E) m_i$$

$$\frac{\partial m_j}{\partial y} = \frac{\alpha_2^{(i)}}{h_E} m_i = \sum_{i=1}^{N_k} (\mathbf{D}_{k,y}^E) m_i$$

$\alpha_1^{(i)}$ and $\alpha_2^{(i)}$ are respectively the coefficients α_1 and α_2 that correspond to the index i, as shown in Tables 3.1 and 3.2. Thus, since $\mathbf{D}_{k,x} = \frac{1}{h_E}\mathbf{D}_{k,x}^E$ and $\mathbf{D}_{k,y} = \frac{1}{h_E}\mathbf{D}_{k,y}^E$, the coefficient matrices are evaluated as follows:

$$(\mathbf{D}_{k,x})_{ij} = \begin{cases} \alpha_1 & \text{if } i = j - \alpha_1 - \alpha_2 \quad \text{and } \alpha_1 > 0, \\ 0 & \text{otherwise} \end{cases}$$

and

$$(\mathbf{D}_{k,y})_{ij} = \begin{cases} \alpha_2 & \text{if } i = j - \alpha_1 - \alpha_2 - 1 \quad \text{and } \alpha_2 > 0, \\ 0 & \text{otherwise} \end{cases}$$

3.1.2 Divergence matrix

Another important tool useful to deal with VEM implementation is the divergence matrix B^E [6]. The local pressure degrees of freedom are represented with respect to the re-scaled basis $\mathbb{M}_{k-1}(E)$:

$$q = \sum_{i=1}^{\pi_{k-1}} c_i \frac{h_E}{|E|} m_i. \tag{3.8}$$

where $\{c_i\}_{i=1}^{\pi_{k-1}}$ are the unknown coefficients of q for each element. π_{k-1} is the dimension of the space $\mathbb{P}_{k-1}$.

From the definition of the divergence moments $\mathbf{D}_V 4$, using the previous relation:

$$\begin{aligned} &\int_E (\text{div } \mathbf{v}_h) m_j \, dE = \frac{|E|}{h_E} \mathbf{D}_V 4(\mathbf{v}_h) \qquad \text{for } j = 2, 3 \\ &\int_E (\text{div } \mathbf{v}_h) \, dE = \int_{\partial E} \mathbf{v}_h \cdot \mathbf{n} \, dE = \sum_{e \in \partial E} \int_e \mathbf{v}_h \cdot \mathbf{n}_e \, dE \qquad \text{for } j = 1 \end{aligned} \tag{3.9}$$

This allows us to exactly evaluate the bilinear form $b(\mathbf{v}, q)$ of the Stokes problem in the local matrix $B^E \subseteq \mathbb{R}^{\dim\left(Q_h^E\right) \times \dim\left(\mathbf{V}_h^E\right)}$.

$$B^E = \left[\begin{array}{ccc|ccc} b_1 & \dots & b_{2kn_E} & 0 & \dots & 0 \\ \hline & \mathbf{0} & & & \mathbf{I} & \end{array}\right] \tag{3.10}$$

where

$$b_i = \frac{h_E}{|E|} \int_{\partial E} \boldsymbol{\varphi}_i \cdot \mathbf{n} \, de \qquad \text{for } i = 1, \dots, 2kn_E.$$

3.2 Projector Π^∇

To compute the discrete VEM bilinear form 3.11 it is necessary to compute the polynomial projection of the basis functions $\Pi_k^\nabla : \mathbf{V}_h^E \to [\mathbb{P}_k(E)]^2$.

$$a_h^{\nabla,E}(\boldsymbol{\varphi_i}, \boldsymbol{\varphi_j}) \coloneqq \int_E \nabla(\Pi_k^\nabla \boldsymbol{\varphi_i}) : \nabla(\Pi_k^\nabla \boldsymbol{\varphi_j}) \, dE + \mathcal{S}^\nabla \left((I - \Pi_k^\nabla)\boldsymbol{\varphi_i}, (I - \Pi_k^\nabla)\boldsymbol{\varphi_j} \right) \tag{3.11}$$

The equation describing the projection operator is as follows [6]:

$$\begin{cases} \displaystyle\int_E \nabla(\mathbf{v}_h - \Pi_k^\nabla \mathbf{v}_h) : \nabla \mathbf{m}_j \, dE = 0 & \forall \mathbf{m}_j \in [\mathbb{M}_k(E)]^2 \setminus [\mathbb{M}_0(E)]^2 \\ \displaystyle\int_{\partial E} (\mathbf{v}_h - \Pi_k^\nabla \mathbf{v}_h) \cdot \mathbf{m}_j \, de = 0 & \forall \mathbf{m}_j \in [\mathbb{M}_0(E)]^2 \end{cases} \tag{3.12}$$

which can be rewrote as:

$$\sum_{i=1}^{2\pi_k} \xi_i \int_E \nabla \mathbf{m}_i : \nabla \mathbf{m}_j \, dE = \int_E \nabla \mathbf{v}_h : \nabla \mathbf{m}_j \, dE. \tag{3.13}$$

From this formulation, it is possible to identify two matrices from the right-hand side term and from the left-hand side term and then evaluate the unknown coefficients ξ_i that represent the projection matrix from $\mathbf{V}_h^E$ to $[\mathbb{P}_k(E)]^2$.

3.2.1 Matrix G

$$G_{ij} = \int_E \nabla \mathbf{m}_i : \nabla \mathbf{m}_j \, dE = \sum_{a \in n_{\text{internal}}} W_a \Big(\nabla \mathbf{m}_i(\hat{\mathbf{x}}_a) : \nabla \mathbf{m}_j(\hat{\mathbf{x}}_a) \Big) \tag{3.14}$$

Where $\hat{\mathbf{x}}_a$ represents the internal Gauss-Lobatto quadrature points.
$\mathbf{m}_i$ basis are defined as follows for $k = 2$:

$$\left\{ \begin{pmatrix} m_i \\ 0 \end{pmatrix} \right\}_{i=1}^{6}, \left\{ \begin{pmatrix} 0 \\ m_i \end{pmatrix} \right\}_{i=1}^{6}$$

And the gradient can be evaluated:

$$\nabla \mathbf{m}_i = \begin{bmatrix} \dfrac{\partial m_{x,i}}{\partial x} & \dfrac{\partial m_{x,i}}{\partial y} \\ \dfrac{\partial m_{y,i}}{\partial x} & \dfrac{\partial m_{y,i}}{\partial y} \end{bmatrix}$$

Table 3.3: m_i basis, gradient and laplacian of m_i for $k = 1$

i	$\mathbf{m}_i$	$\nabla \mathbf{m}_i$	$\Delta \mathbf{m}_i$
1	$\begin{pmatrix} 1 \\ 0 \end{pmatrix}$	$\begin{bmatrix} 0 & 0 \\ 0 & 0 \end{bmatrix}$	$\begin{pmatrix} 0 \\ 0 \end{pmatrix}$
2	$\dfrac{x - x_E}{h_E} \begin{pmatrix} 1 \\ 0 \end{pmatrix}$	$\dfrac{1}{h_E} \begin{bmatrix} 1 & 0 \\ 0 & 0 \end{bmatrix}$	$\begin{pmatrix} 0 \\ 0 \end{pmatrix}$
3	$\dfrac{y - y_E}{h_E} \begin{pmatrix} 1 \\ 0 \end{pmatrix}$	$\dfrac{1}{h_E} \begin{bmatrix} 0 & 1 \\ 0 & 0 \end{bmatrix}$	$\begin{pmatrix} 0 \\ 0 \end{pmatrix}$
4	$\begin{pmatrix} 0 \\ 1 \end{pmatrix}$	$\begin{bmatrix} 0 & 0 \\ 0 & 0 \end{bmatrix}$	$\begin{pmatrix} 0 \\ 0 \end{pmatrix}$
5	$\dfrac{x - x_E}{h_E} \begin{pmatrix} 0 \\ 1 \end{pmatrix}$	$\dfrac{1}{h_E} \begin{bmatrix} 0 & 0 \\ 1 & 0 \end{bmatrix}$	$\begin{pmatrix} 0 \\ 0 \end{pmatrix}$
6	$\dfrac{y - y_E}{h_E} \begin{pmatrix} 0 \\ 1 \end{pmatrix}$	$\dfrac{1}{h_E} \begin{bmatrix} 0 & 0 \\ 0 & 1 \end{bmatrix}$	$\begin{pmatrix} 0 \\ 0 \end{pmatrix}$

Table 3.4: m_i basis, gradient and laplacian of m_i for $k = 2$

i	$\mathbf{m}_i$	$\nabla \mathbf{m}_i$	$\Delta \mathbf{m}_i$
1	$\begin{pmatrix}1\\0\end{pmatrix}$	$\begin{bmatrix}0 & 0\\0 & 0\end{bmatrix}$	$\begin{pmatrix}0\\0\end{pmatrix}$
2	$\frac{x-x_E}{h_E}\begin{pmatrix}1\\0\end{pmatrix}$	$\frac{1}{h_E}\begin{bmatrix}1 & 0\\0 & 0\end{bmatrix}$	$\begin{pmatrix}0\\0\end{pmatrix}$
3	$\frac{y-y_E}{h_E}\begin{pmatrix}1\\0\end{pmatrix}$	$\frac{1}{h_E}\begin{bmatrix}0 & 1\\0 & 0\end{bmatrix}$	$\begin{pmatrix}0\\0\end{pmatrix}$
4	$\frac{(x-x_E)^2}{h_E^2}\begin{pmatrix}1\\0\end{pmatrix}$	$\frac{2(x-x_E)}{h_E^2}\begin{bmatrix}1 & 0\\0 & 0\end{bmatrix}$	$\frac{2}{h_E^2}\begin{pmatrix}1\\0\end{pmatrix}$
5	$\frac{(x-x_E)(y-y_E)}{h_E^2}\begin{pmatrix}1\\0\end{pmatrix}$	$\frac{1}{h_E^2}\begin{bmatrix}(y-y_E) & (x-x_E)\\0 & 0\end{bmatrix}$	$\begin{pmatrix}0\\0\end{pmatrix}$
6	$\frac{(y-y_E)^2}{h_E^2}\begin{pmatrix}1\\0\end{pmatrix}$	$\frac{2(y-y_E)}{h_E^2}\begin{bmatrix}0 & 1\\0 & 0\end{bmatrix}$	$\frac{2}{h_E^2}\begin{pmatrix}1\\0\end{pmatrix}$
7	$\begin{pmatrix}0\\1\end{pmatrix}$	$\begin{bmatrix}0 & 0\\0 & 0\end{bmatrix}$	$\begin{pmatrix}0\\0\end{pmatrix}$
8	$\frac{x-x_E}{h_E}\begin{pmatrix}0\\1\end{pmatrix}$	$\frac{1}{h_E}\begin{bmatrix}0 & 0\\1 & 0\end{bmatrix}$	$\begin{pmatrix}0\\0\end{pmatrix}$
9	$\frac{y-y_E}{h_E}\begin{pmatrix}0\\1\end{pmatrix}$	$\frac{1}{h_E}\begin{bmatrix}0 & 0\\0 & 1\end{bmatrix}$	$\begin{pmatrix}0\\0\end{pmatrix}$
10	$\frac{(x-x_E)^2}{h_E^2}\begin{pmatrix}0\\1\end{pmatrix}$	$\frac{2(x-x_E)}{h_E^2}\begin{bmatrix}0 & 0\\1 & 0\end{bmatrix}$	$\frac{2}{h_E^2}\begin{pmatrix}0\\1\end{pmatrix}$
11	$\frac{(x-x_E)(y-y_E)}{h_E^2}\begin{pmatrix}0\\1\end{pmatrix}$	$\frac{1}{h_E^2}\begin{bmatrix}0 & 0\\(y-y_E) & (x-x_E)\end{bmatrix}$	$\begin{pmatrix}0\\0\end{pmatrix}$
12	$\frac{(y-y_E)^2}{h_E^2}\begin{pmatrix}0\\1\end{pmatrix}$	$\frac{2(y-y_E)}{h_E^2}\begin{bmatrix}0 & 0\\0 & 1\end{bmatrix}$	$\frac{2}{h_E^2}\begin{pmatrix}0\\1\end{pmatrix}$

Thus, the matrix G has two null rows and columns, which pair with the basis functions m_1 and m_7. The last line of Equation 3.12 introduces a new condition to remove null rows. It can be written as:

$$\sum_{i=1}^{2\pi_k} \xi_i \int_{\partial E} \mathbf{m}_i \cdot \mathbf{m}_j \, de = \int_{\partial E} \mathbf{v}_h \cdot \mathbf{m}_j \, de \tag{3.15}$$

where $\pi_k = \dfrac{(k+1)(k+2)}{2}$.

The left-hand side of 3.15:

$$\int_{\partial E} \mathbf{m}_i \cdot \mathbf{m}_j \, de = \sum_{a \in n_{\text{boundary}}} W_a \Big(\mathbf{m}_i(\hat{\mathbf{x}}_a) \cdot \mathbf{m}_j(\hat{\mathbf{x}}_a) \Big)$$

It must be taken into account that $\mathbf{m}_j \in [\mathbb{M}_0(E)]^2$, thus $j = 1{,}7$ for $k = 2$. These are the new contributes to the matrix G:

$$\begin{cases} G_{1:6,1} = \sum_a W_a m_i(\hat{\mathbf{x}}_a) \\ G_{7:12,7} = \sum_a W_a m_i(\hat{\mathbf{x}}_a) \end{cases}$$

Matrix G for $k = 2$ has the following structure:

$$G = \begin{bmatrix} \bullet & \bullet & \bullet & \bullet & \bullet & \bullet & & & & & & \\ & \bullet & & \bullet & \bullet & & & & & & & \\ & & \bullet & & \bullet & \bullet & & & & & & \\ & \bullet & & \bullet & \bullet & & & & & & & \\ & \bullet & \bullet & \bullet & \bullet & \bullet & & & & & & \\ & & \bullet & & \bullet & \bullet & & & & & & \\ & & & & & & \bullet & \bullet & \bullet & \bullet & \bullet & \bullet \\ & & & & & & & \bullet & & \bullet & \bullet & \\ & & & & & & & & \bullet & & \bullet & \bullet \\ & & & & & & & \bullet & & \bullet & \bullet & \\ & & & & & & & \bullet & \bullet & \bullet & \bullet & \bullet \\ & & & & & & & & \bullet & & \bullet & \bullet \end{bmatrix} \tag{3.16}$$

3.2.2 Matrix B

Matrix B represents the right-hand side term in Eq. 3.13:

$$\int_E \nabla \mathbf{v}_h : \nabla \mathbf{m}_j \, dE = -\int_E \mathbf{v}_h \cdot \Delta \mathbf{m}_j \, dE + \sum_{e \in \partial E} \int_e \mathbf{v}_h \cdot (\nabla \mathbf{m}_j \mathbf{n}_e) \, dE \tag{3.17}$$

The boundary summation is easily computable because VEM function in quadrature nodes is $\binom{1}{0}$ or $\binom{0}{1}$.

$$\sum_{e\in\partial E}\int_e \mathbf{v}_h\cdot(\nabla\mathbf{m}_j\mathbf{n}_e)\,dE=\sum_{e\in\partial E}\sum_{a\in n_{\text{boundary}}} W_a\mathbf{v}_i(\hat{\mathbf{x}}_a)\cdot(\nabla\mathbf{m}_j(\hat{\mathbf{x}}_a)\mathbf{n}_e).$$

The following matrix represents the value of the VEM function in all nodes corresponding to the degrees of freedom.

$$\mathbf{v}_i(\hat{\mathbf{x}}_a)=\text{diag}\left(\underbrace{\begin{pmatrix}1\\0\end{pmatrix}}_{\text{node 1}},\underbrace{\begin{pmatrix}1\\0\end{pmatrix}}_{\text{node 2}},\dots,\underbrace{\begin{pmatrix}1\\0\end{pmatrix}}_{\text{node }2n_e},\underbrace{\begin{pmatrix}1\\0\end{pmatrix}}_{\substack{\text{internal}\\\text{node}}},\underbrace{\begin{pmatrix}0\\1\end{pmatrix}}_{\text{node 1}},\underbrace{\begin{pmatrix}0\\1\end{pmatrix}}_{\text{node 2}}\dots,\underbrace{\begin{pmatrix}0\\1\end{pmatrix}}_{\text{node }2n_e},\underbrace{\begin{pmatrix}0\\1\end{pmatrix}}_{\substack{\text{internal}\\\text{node}}}\right) \tag{3.18}$$

the first term of Equation 3.17 can be easily evaluated by rewriting the Laplacian of the basis as a function of another basis, as previously done with the derivative matrix. As shown in Table 3.4, $\Delta\mathbf{m}_j$ is:

$$\Delta\mathbf{m}_4,\Delta\mathbf{m}_6=\Delta\mathbf{m}_{(4,\emptyset)},\Delta\mathbf{m}_{(6,\emptyset)}=\frac{2}{h_E^2}\mathbf{m}_{(1,\emptyset)}$$

and:

$$\Delta\mathbf{m}_{10},\Delta\mathbf{m}_{12}=\Delta\mathbf{m}_{(\emptyset,4)},\Delta\mathbf{m}_{(\emptyset,6)}=\frac{2}{h_E^2}\mathbf{m}_{(\emptyset,1)}.$$

Thus, it becomes:

$$\int_E\mathbf{v}_h\cdot\Delta\mathbf{m}_4\,dE=\frac{2}{h_E^2}\int_E\mathbf{v}_h\cdot\mathbf{m}_{(1,\emptyset)}\,dE=\frac{2}{h_E}\int_E\mathbf{v}_h\cdot\nabla m_2\,dE$$

$$\int_E\mathbf{v}_h\cdot\nabla m_2\,dE=-\int_E(\text{div}\mathbf{v}_h)m_2\,dE+\sum_{e\in\partial E}\int_e(\mathbf{v}_h\cdot\mathbf{n}_e)m_2\,de \tag{3.19}$$

The same steps are used for $j=6,10,12$.

To evaluate the first integral of Equation 3.19 it is necessary to exploit the basis

decomposition in Table 3.5 and the local matrix B^E (Subsection 3.1.2):

$$\begin{bmatrix} \begin{bmatrix} \\ \\ \\ \\ \\ \end{bmatrix}, \overbrace{\begin{bmatrix} \\ \\ \frac{2|E|}{h_E^2} \\ \frac{2|E|}{h_E^2} \\ \\ \\ \end{bmatrix}}^{kN_E+1}, \begin{bmatrix} \\ \\ \\ \\ \\ \end{bmatrix}, \overbrace{\begin{bmatrix} \\ \\ \\ \\ \frac{2|E|}{h_E^2} \\ \frac{2|E|}{h_E^2} \end{bmatrix}}^{2(kN_E+1)} \end{bmatrix} \tag{3.20}$$

Solving the summation (3.19), we obtain:

$$-\frac{2}{h_E}\begin{bmatrix}\begin{bmatrix} \\ \\ n_{ex}W_1m_2(\hat{\mathbf{x}}_1) & \dots & n_{ex}W_{kN_E}m_2(\hat{\mathbf{x}}_{kN_E}) \\ n_{ex}W_1m_2(\hat{\mathbf{x}}_1) & \dots & n_{ex}W_{kN_E}m_2(\hat{\mathbf{x}}_{kN_E}) \\ \\ \\ \\ \end{bmatrix}, \begin{bmatrix}\end{bmatrix}, \begin{bmatrix} \\ \\ \\ \\ \\ \\ n_{ey}W_1m_3(\hat{\mathbf{x}}_1) & \dots & n_{ey}W_{kN_E}m_3(\hat{\mathbf{x}}_{kN_E}) \\ n_{ey}W_1m_3(\hat{\mathbf{x}}_1) & \dots & n_{ey}W_{kN_E}m_3(\hat{\mathbf{x}}_{kN_E}) \end{bmatrix}, \begin{bmatrix}\end{bmatrix}\end{bmatrix} \tag{3.21}$$

The right-hand side term of Equation 3.15 is:

$$\int_{\partial E} \mathbf{v}_h \cdot \mathbf{m}_j \, de = \sum_{a \in n_{\text{bordo}}} W_a \mathbf{v}_i(\hat{\mathbf{x}}_a) \cdot \mathbf{m}_j(\hat{\mathbf{x}}_a)$$

where $j = 1{,}7$ for $k = 2$.

Matrix B is the sum of these four contributions and takes this form:

$$B = \left[\begin{bmatrix} \bullet & \bullet & \bullet & \dots & \bullet & \bullet & \bullet \\ \bullet & \bullet & \bullet & \dots & \bullet & \bullet & \bullet \\ \bullet & \bullet & \bullet & \dots & \bullet & \bullet & \bullet \\ \bullet & \bullet & \bullet & \dots & \bullet & \bullet & \bullet \\ \bullet & \bullet & \bullet & \dots & \bullet & \bullet & \bullet \\ \bullet & \bullet & \bullet & \dots & \bullet & \bullet & \bullet \\ & & & & & & \end{bmatrix}, \begin{bmatrix} \\ \\ \\ \\ \bullet \\ \bullet \\ \\ \\ \\ \\ \\ \\ \end{bmatrix}, \begin{bmatrix} & & & & & & \\ & & & & & & \\ & & & & & & \\ & & & & & & \\ & & & & & & \\ & & & & & & \\ \bullet & \bullet & \bullet & \dots & \bullet & \bullet & \bullet \\ \bullet & \bullet & \bullet & \dots & \bullet & \bullet & \bullet \\ \bullet & \bullet & \bullet & \dots & \bullet & \bullet & \bullet \\ \bullet & \bullet & \bullet & \dots & \bullet & \bullet & \bullet \\ \bullet & \bullet & \bullet & \dots & \bullet & \bullet & \bullet \\ \bullet & \bullet & \bullet & \dots & \bullet & \bullet & \bullet \end{bmatrix}, \begin{bmatrix} \\ \\ \\ \\ \\ \\ \\ \bullet \\ \bullet \end{bmatrix}\right] \tag{3.22}$$

Table 3.5: b_s and β_s coefficients

$\mathbf{m}_{\boldsymbol{\alpha},\emptyset} = \frac{h}{\lvert\boldsymbol{\alpha}\rvert+1}\nabla m_{(\alpha_1+1,\alpha_2)} + \frac{\alpha_2}{\lvert\boldsymbol{\alpha}\rvert+1}\mathbf{m}^{\perp} m_{(\alpha_1,\alpha_2-1)}$
$\mathbf{m}_{\emptyset,\boldsymbol{\beta}} = \frac{h}{\lvert\boldsymbol{\beta}\rvert+1}\nabla m_{(\beta_1,\beta_2+1)} - \frac{\beta_1}{\lvert\boldsymbol{\beta}\rvert+1}\mathbf{m}^{\perp} m_{(\beta_1-1,\beta_2)}$
$\mathbf{m}_{1,\emptyset} = h\nabla m_{(1,0)} = h\nabla m_2$
$\mathbf{m}_{2,\emptyset} = \frac{h}{2}\nabla m_{(2,0)} = \frac{h}{2}\nabla m_4$
$\mathbf{m}_{3,\emptyset} = \frac{h}{2}\nabla m_{(1,1)} + \frac{1}{2}\mathbf{m}^{\perp} m_{(0,0)} = \frac{h}{2}\nabla m_5 + \frac{1}{2}\mathbf{m}^{\perp} m_1$
$\mathbf{m}_{4,\emptyset} = \frac{h}{3}\nabla m_{(3,0)} = \frac{h}{3}\nabla m_7$
$\mathbf{m}_{5,\emptyset} = \frac{h}{3}\nabla m_{(2,1)} + \frac{1}{3}\mathbf{m}^{\perp} m_{(1,0)} = \frac{h}{3}\nabla m_8 + \frac{1}{3}\mathbf{m}^{\perp} m_2$
$\mathbf{m}_{6,\emptyset} = \frac{h}{3}\nabla m_{(1,2)} + \frac{2}{3}\mathbf{m}^{\perp} m_{(0,1)} = \frac{h}{3}\nabla m_9 + \frac{2}{3}\mathbf{m}^{\perp} m_3$
$\mathbf{m}_{\emptyset,1} = h\nabla m_{(0,1)} = h\nabla m_3$
$\mathbf{m}_{\emptyset,2} = \frac{h}{2}\nabla m_{(1,1)} - \frac{1}{2}\mathbf{m}^{\perp} m_{(0,0)} = \frac{h}{2}\nabla m_5 + \frac{1}{2}\mathbf{m}^{\perp} m_1$
$\mathbf{m}_{\emptyset,3} = \frac{h}{2}\nabla m_{(0,2)} = \frac{h}{2}\nabla m_6$
$\mathbf{m}_{\emptyset,4} = \frac{h}{3}\nabla m_{(2,1)} - \frac{2}{3}\mathbf{m}^{\perp} m_{(1,0)} = \frac{h}{3}\nabla m_8 - \frac{2}{3}\mathbf{m}^{\perp} m_2$
$\mathbf{m}_{\emptyset,5} = \frac{h}{3}\nabla m_{(1,2)} - \frac{1}{3}\mathbf{m}^{\perp} m_{(0,1)} = \frac{h}{3}\nabla m_9 - \frac{1}{3}\mathbf{m}^{\perp} m_3$
$\mathbf{m}_{\emptyset,6} = \frac{h}{3}\nabla m_{(0,3)} = \frac{h}{2}\nabla m_{10}$

3.3 Projector Π^0

In order to obtain the local system of the Stokes problem with the VEM it is necessary to follow another step. To calculate an approximation of the right-hand side term in Equation 2.1 we have to introduce the projector Π_k^0 which provides a L^2-projection from $\mathbf{V}_h^E$ to $[\mathbb{P}_k(E)]^2$. This projector allows us to evaluate the forcing vector in the degrees of freedom and therefore to be able to construct the rhs in the local system. For this purpose, the procedure described in Section 2.5 has been followed. The Π_k^0 projector is defined as follows:

$$\int_E (\mathbf{v}_h - \Pi_k^0 \mathbf{v}_h) \cdot \mathbf{m}_j \, dE = 0 \qquad \forall \mathbf{m}_j \in [\mathbb{M}_k(E)]^2 \tag{3.23}$$

By separating the two products it is possible to rewrite it in this way:

$$\sum_{i=1}^{2\pi_k} \zeta_i \int_E \mathbf{m}_i \cdot \mathbf{m}_j \, dE = \int_E \mathbf{v}_h \cdot \mathbf{m}_j \, dE \tag{3.24}$$

We separate the two contributions on the right and on the left which are evaluated through the construction of the matrices C and H.

3.3.1 Matrix C

The evaluation of the matrix C is simple and follows the same steps used for the matrix G, with the difference that to evaluate the matrix G it is necessary to integrate the Vandermonde matrices of the derivatives of the monomial basis, while for the matrix C the Vandermonde matrix of the basis is used.

The integral is solved by the Gauss quadrature method:

$$\int_E \mathbf{m}_i \cdot \mathbf{m}_j \, dE = \sum_{a \in n_{\text{internal}}} W_a \left(\mathbf{m}_i(\hat{\mathbf{x}}_a) \cdot \mathbf{m}_j(\hat{\mathbf{x}}_a) \right)$$

The matrix C is the following:

$$C = \sum_{a \in n_{\text{internal}}} W_a \left(\mathbf{m}_i(\hat{\mathbf{x}}_a) \cdot \mathbf{m}_j(\hat{\mathbf{x}}_a) \right) \qquad \text{for } i, j = 1, \ldots, 2\pi_k \tag{3.25}$$

3.3.2 Matrix H

The rhs of the Equation 3.24 is equal to:

$$\int_E \mathbf{v}_h \cdot \mathbf{m}_j \, dE = b_1 \underbrace{\int_E \mathbf{v}_h \cdot \nabla m_{\beta_1} \, dE}_{\textbf{(A)}} + b_2 \underbrace{\int_E \mathbf{v}_h \cdot \mathbf{m}^{\perp} m_{\beta_2} \, dE}_{\textbf{(B)}} \tag{3.26}$$

The integral **(A)** can be written as:

$$\int_E \mathbf{v}_h \cdot \nabla m_{\beta_1}\, dE = -\int_E (\text{div } \mathbf{v}_h) m_{\beta_1}\, dE + \sum_{e\in\partial E} \int_e (\mathbf{v}_h \cdot \mathbf{n}_e) m_{\beta_1}\, de \tag{3.27}$$

While the summation is easily computable because the VEM functions are known at the boundary,

$$\sum_{e\in\partial E} \int_e (\mathbf{v}_h \cdot \mathbf{n}_e) m_{\beta_1}\, dE = \sum_{e\in\partial E} \sum_{a\in n_{\text{boundary}}} W_a (\mathbf{v}_i(\hat{\mathbf{x}}_a) \cdot \mathbf{n}_e) m_{\beta_1} \tag{3.28}$$

the moment of the divergence has a more complicated calculation. The Section 3.1.2 can be used to evaluate this integral, for which it is necessary to exploit an order of integration greater than that used for the other integrals because the coefficient β_1, which follows Table 3.5, reaches π_{k+1}.

The integral **(B)**, if $k-2 \leq |\beta_2| \leq k-1$, can be written as:

$$\int_E \mathbf{v}_h \cdot \mathbf{m}^\perp m_{\beta_2}\, dE = \int_E \Pi_k^\nabla \mathbf{v}_h \cdot \mathbf{m}^\perp m_{\beta_2}\, dE = \sum_{i=1}^{2\pi_k} \zeta_i \int_E \mathbf{m}_i \cdot \mathbf{m}^\perp m_{\beta_2}\, dE \tag{3.29}$$

In which the enhancing condition is exploited to evaluate an approximate solution of the integral. The coefficients β_2 come from Table 3.5, which corresponds to:

$$\sum_{a=n_{\text{internal}}} \begin{bmatrix} 0 & 0 & \dots & 0 \\ 0 & 0 & \dots & 0 \\ (\Pi_k^\nabla)_{3,1}\mathbf{m}_3 m_1(\hat{\mathbf{x}}_a) & (\Pi_k^\nabla)_{3,2}\mathbf{m}_3 m_1(\hat{\mathbf{x}}_a) & \dots & (\Pi_k^\nabla)_{3,N_{\text{dof}}}\mathbf{m}_3 m_1(\hat{\mathbf{x}}_a) \\ 0 & 0 & \dots & 0 \\ (\Pi_k^\nabla)_{5,1}\mathbf{m}_5 m_2(\hat{\mathbf{x}}_a) & (\Pi_k^\nabla)_{5,2}\mathbf{m}_5 m_2(\hat{\mathbf{x}}_a) & \dots & (\Pi_k^\nabla)_{5,N_{\text{dof}}}\mathbf{m}_5 m_2(\hat{\mathbf{x}}_a) \\ 0 & 0 & \dots & 0 \\ \vdots & \vdots & & \vdots \\ 0 & 0 & \dots & 0 \\ (\Pi_k^\nabla)_{11,1}\mathbf{m}_{11} m_3(\hat{\mathbf{x}}_a) & (\Pi_k^\nabla)_{11,2}\mathbf{m}_{11} m_3(\hat{\mathbf{x}}_a) & \dots & (\Pi_k^\nabla)_{11,N_{\text{dof}}}\mathbf{m}_{11} m_3(\hat{\mathbf{x}}_a) \\ 0 & 0 & \dots & 0 \end{bmatrix} \cdot \mathbf{m}^\perp(\hat{\mathbf{x}}_a) \tag{3.30}$$

where

$$\mathbf{m}^\perp := \begin{pmatrix} m_{(0,1)} \\ -m_{(1,0)} \end{pmatrix} = \begin{pmatrix} m_3 \\ -m_2 \end{pmatrix}.$$

3.4 Local system

The local stiffness matrix can be evaluated following [2]. Assuming that:

$$\mathbf{v}_h = \sum_{i=1}^{N_{\text{dof}}} \text{dof}_i(\mathbf{v}_h) \boldsymbol{\varphi}_i \qquad \forall\, \mathbf{v}_h \in \mathbf{V}_h^E$$

where $\boldsymbol{\varphi}_i$ represent the basis functions of the space $\mathbf{V}_h^E$ and

$$\mathrm{dof}_i(\boldsymbol{\varphi}_i) = \delta_{ij} \qquad i,j = 1,\dots,N_{\mathrm{dof}},$$

the local stiffness matrix K_E can be computed as:

$$(\mathbf{K}_E)_{ij} = (\nabla\boldsymbol{\varphi}_i, \nabla\boldsymbol{\varphi}_j)_{0,E} \qquad i,j = 1,\dots,N_{\mathrm{dof}} \tag{3.31}$$

To evaluate this integral no quadrature formulas are used which would require approximate forms of the basis functions. The VEM approach requires using the associated bilinear form which is exact if one of the two entries is a polynomial of degree k.

For this reason it is not necessary to write an explicit form of the base function $\boldsymbol{\varphi}_i$.

Using the projector Π^∇ it is possible to write:

$$(\mathbf{K}_E)_{ij} = (\nabla\,\Pi^\nabla\boldsymbol{\varphi}_i, \nabla\,\Pi^\nabla\boldsymbol{\varphi}_j)_{0,E} + \Big(\nabla\,(\mathbf{I}-\Pi^\nabla)\boldsymbol{\varphi}_i, \nabla\,(\mathbf{I}-\Pi^\nabla)\boldsymbol{\varphi}_j\Big)_{0,E} \tag{3.32}$$

The first term assure condition **A2.1** which takes *consistency* while the second term assures condition **A2.2** which takes *stability*.

The following equation is the matrix expression of the local stiffness matrix:

$$\mathbf{K}_E^h = (\Pi_*^\nabla)^T\tilde{G}(\Pi_*^\nabla) + (\mathbf{I}-\Pi^\nabla)^T(\mathbf{I}-\Pi^\nabla) \tag{3.33}$$

where $\tilde{G}$ coincides with G except for the rows depending on the monomial base m_1 which is set to zero. For $k=2$ the rows set to zero are the first and the seventh because: $\mathbf{m}_1 = \binom{m_1}{0}$ and $\mathbf{m}_7 = \binom{0}{m_1}$.

Then:

$$\Pi_*^\nabla = G^{-1}B$$

and

$$\Pi^\nabla = D\,\Pi_*^\nabla.$$

The matrix D represents the value of the degrees of freedom calculated in the monomial basis:

$$D = \begin{bmatrix} \mathrm{dof}_1(\mathbf{m}_1) & \mathrm{dof}_1(\mathbf{m}_2) & \dots & \mathrm{dof}_1(\mathbf{m}_{2\pi_k}) \\ \mathrm{dof}_2(\mathbf{m}_1) & \mathrm{dof}_1(\mathbf{m}_2) & \dots & \mathrm{dof}_1(\mathbf{m}_{2\pi_k}) \\ \vdots & \vdots & \ddots & \vdots \\ \mathrm{dof}_{N^{\mathrm{dof}}}(\mathbf{m}_1) & \mathrm{dof}_{N^{\mathrm{dof}}}(\mathbf{m}_2) & \dots & \mathrm{dof}_{N^{\mathrm{dof}}}(\mathbf{m}_{2\pi_k}) \end{bmatrix} \tag{3.34}$$

For $k=2$ the matrix D has two diagonal blocks that include the boundary Vandermonde matrix and two rows that correspond to the $\mathbf{D}_V4$ degrees of freedom that represent the integral of the divergence of the basis multiplied by the column 2 or 3 respectively of the Vandermonde matrix.

For $k=1$ there are no $\mathbf{D}_V4$ degrees of freedom.

3.5 Global system

Once the local system has been evaluated, the contributions are saved within a vector which, when suitably indexed, allows the construction of the global stiffness matrix. The local stiffness matrix of each element is a diagonal block matrix composed of two blocks, where the first block refers to the degrees of freedom of $\mathbf{u}_x$ and the second to $\mathbf{u}_y$. By exploiting the decoupling of the system, it is possible to separately assemble the global matrix by two blocks that refers to the $\mathbf{u}_x$ and $\mathbf{u}_y$ degrees of freedom.

The global system also requires some coupling terms between velocity and pressure, which correspond to the exact solution of the bilinear form $b(\mathbf{v}_h, q)$, that we have already calculated in Section 3.1.2 within the matrix B_E, built starting from $\mathbf{D}_V 4$.

We have introduced a new set of global basis functions $\varphi_j^{i_j}$ in order to write an algebraic formulation of the Stoke Problem in the cases or our interest. j represents the number of the set of degrees of freedom.

- $\varphi_1^{i_1}$, corresponding to $\mathbf{D}_V 1$, $i_1 = 1, \dots, 2n_V$
- $\varphi_2^{i_2}$, corresponding to $\mathbf{D}_V 2$, $i_1 = 1, \dots, 2(k-1)n_E$
- $\varphi_3^{i_3}$, corresponding to $\mathbf{D}_V 3$, $i_1 = 1, \dots, n_P \frac{(k-1)(k-2)}{2}$
- $\varphi_4^{i_4}$, corresponding to $\mathbf{D}_V 4$, $i_1 = 1, \dots, n_P(\frac{(k+1)k}{2} - 1)$

Here, the set $\left\{ \varphi_1^{i_1}, \varphi_2^{i_2}, \varphi_3^{i_3}, \varphi_4^{i_4} \;\middle|\; i_1, i_2, i_3, i_4 \right\}$ is a basis for $\mathbf{V}_h$.

The global stiffness matrix $\mathbf{S}$ is defined as the evaluation of the bilinear form $a_h(\varphi_j^{i_j}, \varphi_l^{i_l})$:

$$(\mathbf{S})_{i_j, i_l} := (S_{j,k})_{i_j, i_l} = a_h(\varphi_j^{i_j}, \varphi_l^{i_l}) \qquad \text{for } j, l = 1, ..., 4 \tag{3.35}$$

and the matrix $\mathbf{B}$ as the evaluation of the exact bilinear form $b(\varphi_j^{i_j}, m_\alpha)$:

$$(\mathbf{B})_{\alpha, i_j} := b(\varphi_j^{i_j}, m_\alpha) \qquad \text{for } |\boldsymbol{\alpha}| = 0, ..., k \text{ and } j = 1, ..., 4 \tag{3.36}$$

The matrix form for the Stokes problem is the following:

$$\left[\begin{array}{cccc|cc} S_{11} & S_{12} & S_{13} & S_{14} & B_1^T & 0 \\ S_{12}^T & S_{22} & S_{23} & S_{24} & B_2^T & 0 \\ S_{13}^T & S_{23}^T & S_{33} & S_{34} & 0 & 0 \\ S_{14}^T & S_{24}^T & S_{34}^T & S_{44} & 0 & I \\ \hline B_1 & B_2 & 0 & 0 & 0 & 0 \\ 0 & 0 & 0 & I & 0 & 0 \end{array}\right] \left[\begin{array}{c} \mathbf{u}_1 \\ \mathbf{u}_2 \\ \mathbf{u}_3 \\ \mathbf{u}_4 \\ \hline p_0 \\ p^\perp \end{array}\right] = \left[\begin{array}{c} \mathbf{f}_{h,1} \\ \mathbf{f}_{h,2} \\ \mathbf{f}_{h,3} \\ \mathbf{f}_{h,4} \\ \hline 0 \\ 0 \end{array}\right] \tag{3.37}$$

Subsequently, the stiffness matrix has been ordered to distinguish two non-zero blocks on the diagonal, as follows:

$$\left[\begin{array}{ccc|ccc|cc} S_{11,x} & S_{12,x} & S_{14,x} & 0 & 0 & 0 & B_{1,x}^T & 0 \\ S_{12,x}^T & S_{22,x} & S_{24,x} & 0 & 0 & 0 & B_{2,x}^T & 0 \\ S_{14,x}^T & S_{24,x}^T & S_{44,x} & 0 & 0 & 0 & 0 & I \\ \hline 0 & 0 & 0 & S_{11,y} & S_{12,y} & S_{14,y} & B_{1,y}^T & 0 \\ 0 & 0 & 0 & S_{12,y}^T & S_{22,y} & S_{24,y} & B_{2,y}^T & 0 \\ 0 & 0 & 0 & S_{14,y}^T & S_{24,y}^T & S_{44,y} & 0 & I \\ \hline B_{1,x} & B_{2,x} & 0 & B_{1,y} & B_{2,y} & 0 & 0 & 0 \\ 0 & 0 & I & 0 & 0 & I & 0 & 0 \end{array}\right] \left[\begin{array}{c} \mathbf{u}_{1,x} \\ \mathbf{u}_{2,x} \\ \mathbf{u}_{4,x} \\ \hline \mathbf{u}_{1,y} \\ \mathbf{u}_{2,y} \\ \mathbf{u}_{4,y} \\ \hline p_0 \\ p^{\perp} \end{array}\right] = \left[\begin{array}{c} \mathbf{f}_{h,1,x} \\ \mathbf{f}_{h,2,x} \\ \mathbf{f}_{h,4,x} \\ \hline \mathbf{f}_{h,1,y} \\ \mathbf{f}_{h,2,y} \\ \mathbf{f}_{h,4,y} \\ \hline 0 \\ 0 \end{array}\right] \tag{3.38}$$

where $\mathbf{u}_{i,x}$ and $\mathbf{u}_{i,y}$ represent respectively the x-components and the y-components of the vector $\mathbf{u}_i$.

To evaluate the system for $k = 1$ it is necessary to take into account that the only degrees of freedom of the problem are those $\mathbf{D}_V 1$ and $\mathbf{D}_Q$. The global system looks like this:

$$\left[\begin{array}{cc|c} S_{11,x} & 0 & B_{1,x}^T \\ 0 & S_{11,y} & B_{1,y}^T \\ \hline B_{1,x} & B_{1,y} & 0 \end{array}\right] \left[\begin{array}{c} \mathbf{u}_{1,x} \\ \mathbf{u}_{1,y} \\ \hline p_0 \end{array}\right] = \left[\begin{array}{c} \mathbf{f}_{h,1,x} \\ \mathbf{f}_{h,1,y} \\ \hline 0 \end{array}\right] \tag{3.39}$$

Chapter 4

The Reduced Problem

This method has an important advantage that makes it very efficient in terms of number of degrees of freedom. By selecting the degrees of freedom as done in 2.3, an orthogonality condition is verified among many pressure degrees of freedom and the associated degrees of freedom for the velocities.

Therefore, several degrees of freedom can be eliminated from the system to obtain a new reduced problem with fewer degrees of freedom.

The reduced virtual element discretization of the Stokes Problem (1.16) is:

$$\begin{cases} \text{find } \hat{\mathbf{u}}_h \in \hat{\mathbf{V}}_h \text{ and } \hat{p}_h \in \hat{Q}_h, \text{ such that} & \\ a_h(\hat{\mathbf{u}}_h, \hat{\mathbf{v}}_h) + b(\hat{\mathbf{v}}_h, \hat{p}_h) = (\mathbf{f}_h, \hat{\mathbf{v}}_h) & \text{for all } \hat{\mathbf{v}}_h \in \hat{\mathbf{V}}_h, \\ b(\hat{\mathbf{u}}_h, \hat{q}_h) = 0 & \text{for all } \hat{q}_h \in \hat{Q}_h. \end{cases} \tag{4.1}$$

where $\hat{\mathbf{V}}_h \subseteq \mathbf{V}_h$ with all the divergence moment degrees of freedom $\mathbf{D}_V 4$ set to zero and $\hat{Q}_h \subseteq Q_h$ is the space of constant functions for each elements.

$$\hat{\mathbf{V}}_h := \left\{ \mathbf{v} \in [H_0^1(\Omega)]^2 \quad \text{s.t.} \quad \mathbf{v}|_K \in \hat{\mathbf{V}}_h^K \quad \text{for all } K \in \mathcal{T}_h \right\} \tag{4.2}$$

$$\hat{Q}_h := \left\{ q \in L_0^2(\Omega) \quad \text{s.t.} \quad q|_K \in \hat{Q}_h^K \quad \text{for all } K \in \mathcal{T}_h \right\} \tag{4.3}$$

And their dimensions are:

$$\dim(\hat{\mathbf{V}}_h) = n_P \frac{(k-1)(k-2)}{2} + 2(n_V + (k-1)n_E)$$

$$\dim(\hat{Q}_h) = n_P - 1$$

If $\mathbf{u}_h \in \mathbf{V}_h$ and $p_h \in Q_h$ are the solution of (1.16) and if $\hat{\mathbf{u}}_h \in \hat{\mathbf{V}}_h$ and $\hat{p}_h \in \hat{Q}_h$ are the solution of (4.1), for all $E \in \mathcal{T}_h$ it is easily proved that:

$$\hat{\mathbf{u}}_h = \mathbf{u}_h \tag{4.4}$$

and

$$\hat{p}_{h|E} = \Pi_0^{0,E} p_h \tag{4.5}$$

To implement the Reduced Problem we have used the coefficients matrix of the complete problem to which the extra degrees of freedom have been removed, then the rows and columns of the corresponding degrees of freedom have been simply deleted. By doing so, solving the reduced problem becomes easier because it is not necessary to evaluate new projectors and a smaller global matrix has been obtained.

The reduced problem lessens the number of degrees of freedom, both for pressure and velocity.

As for the pressure, which previously belonged to the space of polynomials of degree $k-1$, in this problem is considered as a constant, with a saving in the number of degrees of freedom equal to:

$$n_P(\dim(\mathbb{P}_{k-1}) - \dim(\mathbb{P}_0)) = n_P \left(\frac{k(k+1)}{2} - 1 \right)$$

The pressure, represented by the polynomial basis described above (Equation 3.1), was considered up to the order $k-1$. In this problem the pressure is a constant, defined in the space $\hat{\mathcal{M}}_0$:

$$\hat{\mathcal{M}}_0 := \{m_0^E \qquad \text{for } E \in \mathcal{T}_h\}$$

that is a basis for $\hat{Q}_h$.

Regarding velocity, the degrees of freedom $\mathbf{D}_V 4$ are removed and this is the number of the dropped velocity global degrees of freedom:

$$n_P(\dim(\mathbb{P}_{k-1}) - 1) = n_P \left(\frac{k(k+1)}{2} - 1 \right)$$

The total saving is:

$$n_P \left(k(k+1) - 2 \right)$$

Table 4.1: Percentage of saving in degrees of freedom for the reduced problem with respect to the original problem

	Voronoi tessellations, Fig. 5.3
% velocity DoFs	17%
% pressure DoFs	67%
% total DoFs	27%

The following line represents the matrix form of the Reduced Problem. It has been evaluated stating from the System 3.37.

$$\left[\begin{array}{ccc|c} S_{11} & S_{12} & S_{13} & B_1^T \\ S_{12}^T & S_{22} & S_{23} & B_2^T \\ S_{13}^T & S_{23}^T & S_{33} & 0 \\ \hline B_1 & B_2 & 0 & 0 \end{array}\right] \left[\begin{array}{c} \hat{\mathbf{u}}_1 \\ \hat{\mathbf{u}}_2 \\ \hat{\mathbf{u}}_3 \\ \hline \hat{p}_0 \end{array}\right] = \left[\begin{array}{c} \mathbf{f}_{h,1} \\ \mathbf{f}_{h,2} \\ \mathbf{f}_{h,3} \\ \hline 0 \end{array}\right] \tag{4.6}$$

Following what has been done in Equation 3.38 it is possible to write:

$$\left[\begin{array}{cc|cc|c} S_{11,x} & S_{12,x} & 0 & 0 & B_{1,x}^T \\ S_{12,x}^T & S_{22,x} & 0 & 0 & B_{2,x}^T \\ \hline 0 & 0 & S_{11,y} & S_{12,y} & B_{1,y}^T \\ 0 & 0 & S_{12,y}^T & S_{22,y} & B_{2,y}^T \\ \hline B_{1,x} & B_{2,x} & B_{1,y} & B_{2,y} & 0 \end{array}\right] \left[\begin{array}{c} \hat{\mathbf{u}}_{1,x} \\ \hat{\mathbf{u}}_{2,x} \\ \hline \hat{\mathbf{u}}_{1,y} \\ \hat{\mathbf{u}}_{2,y} \\ \hline \hat{p}_0 \end{array}\right] = \left[\begin{array}{c} \mathbf{f}_{h,1,x} \\ \mathbf{f}_{h,2,x} \\ \hline \mathbf{f}_{h,1,y} \\ \mathbf{f}_{h,2,y} \\ \hline 0 \end{array}\right] \tag{4.7}$$

Subsequently, the System 4.7 has been solved and a solution equal to that of the original problem has been obtained. For this reason, in the next chapter, in which numerical examples will be presented, the solution for the complete and the reduced system will be indistinctly called solutions of the system of order $k = 2$.

Chapter 5

Numerical results

To perform the numerical tests, a simple square domain $\Omega : [0,1] \times [0,1]$ has been chosen. The proposed method has been tested on different meshes to prove its goodness to find a solution also in the case of very various elements, with different number of edges and area or with a very high aspect ratio.

Here are some of the meshes tested (Figures 5.1, 5.2):

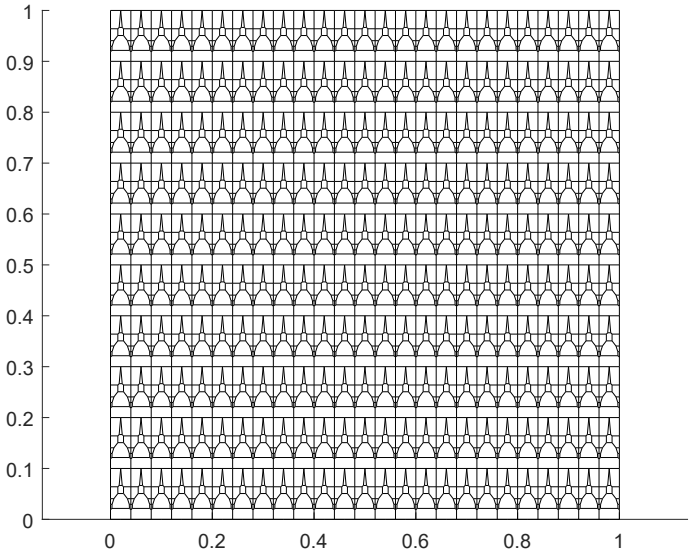

Figure 5.1: Mole mesh

To verify the convergence of the method it was decided to construct a Voronoi tessellation with the PolyMesher software [8], to which an increasing number of elements was set (Figure 5.3).

The load term $\mathbf{f}$ has been chosen in such a way that the exact solution is:

$$\mathbf{u}(x,y) = \begin{pmatrix} \frac{1}{2}\sin(2\pi x)\sin(2\pi x)\sin(2\pi y)\cos(2\pi y) \\ -\frac{1}{2}\sin(2\pi y)\sin(2\pi y)\sin(2\pi x)\cos(2\pi x) \end{pmatrix} \tag{5.1}$$

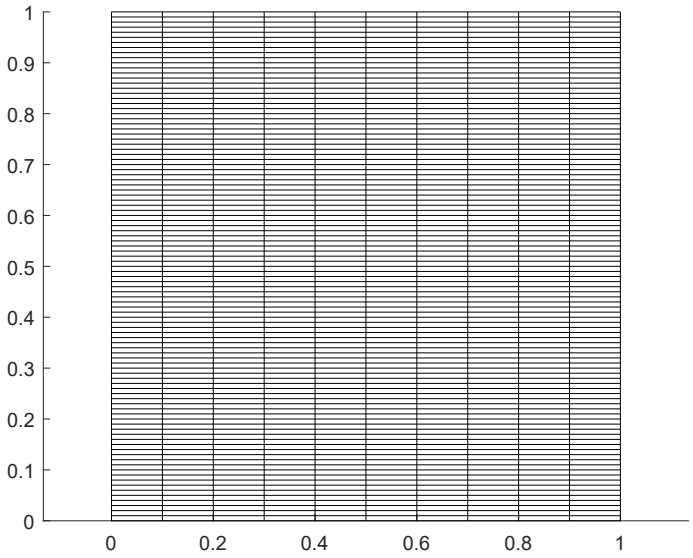

Figure 5.2: Rectangles 10×100 mesh

and

$$p(x, y) = \sin(2\pi x)\ \cos(2\pi y). \tag{5.2}$$

The graphs below (Fig. 5.4-5.9) show the results obtained from applying the method to the meshes that have been shown so far. The pressure field has been represented as a color scale corresponding to the pressure value at the centroid of each cell. After, the velocity field is represented through the velocity vector corresponding to each vertex. The exact speed vector, in orange, and the approximate one, in blue, have been superimposed.

The results are shown only for the case $k = 2$, because graphs with the results for $k = 1$ are not appreciably different.

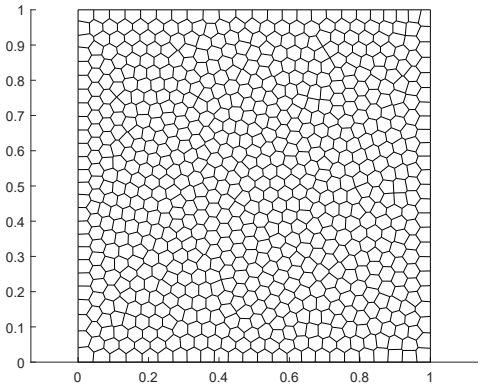

(a) 750 elements

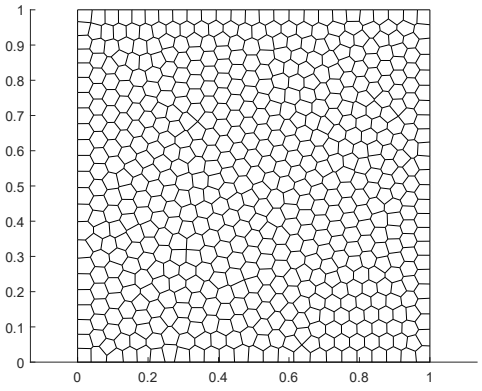

(b) 600 elements

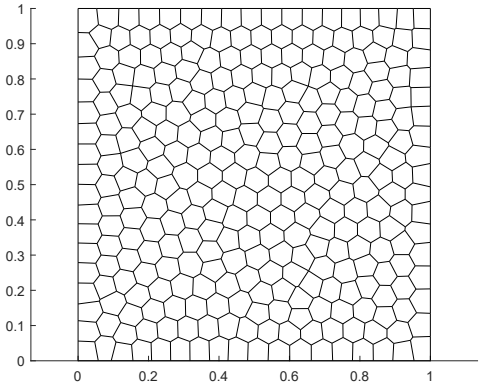

(c) 300 elements

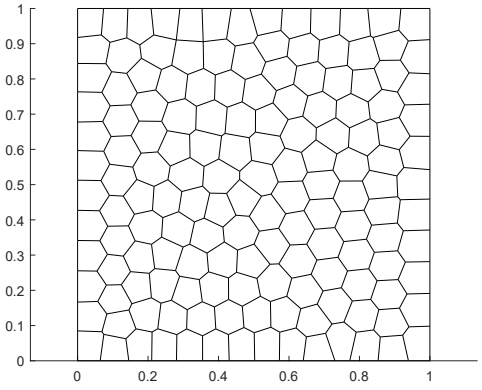

(d) 150 Elements

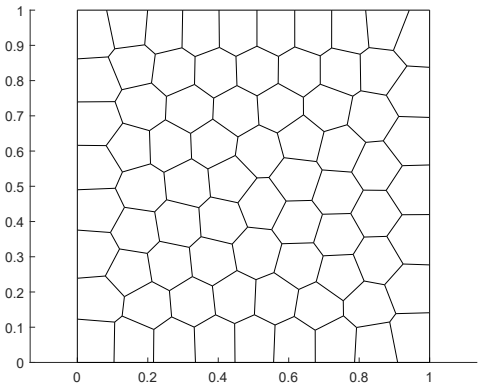

(e) 75 Elements

Figure 5.3: Voronoi tessellations

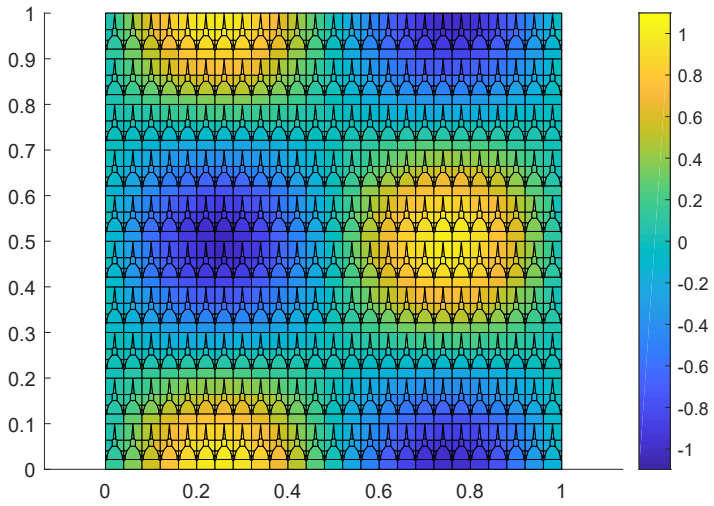

Figure 5.4: Mole pressure field

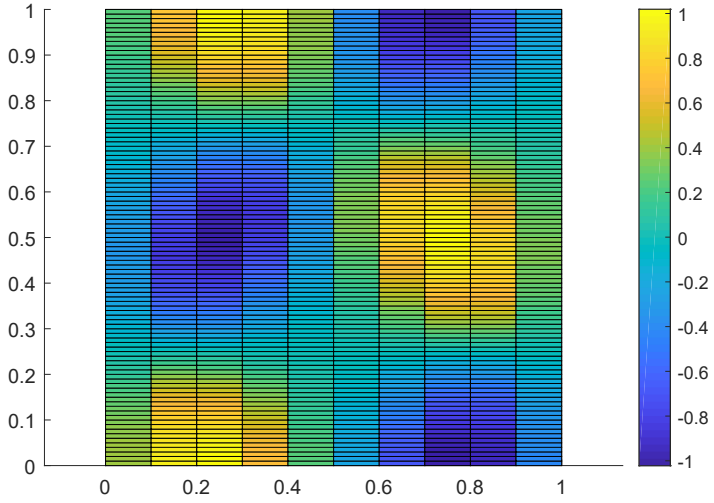

Figure 5.5: Rectangles pressure field

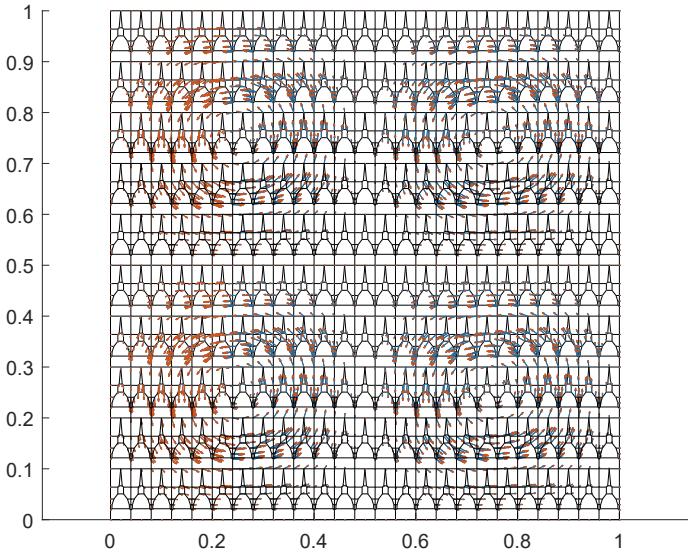

Figure 5.6: Mole velocity field

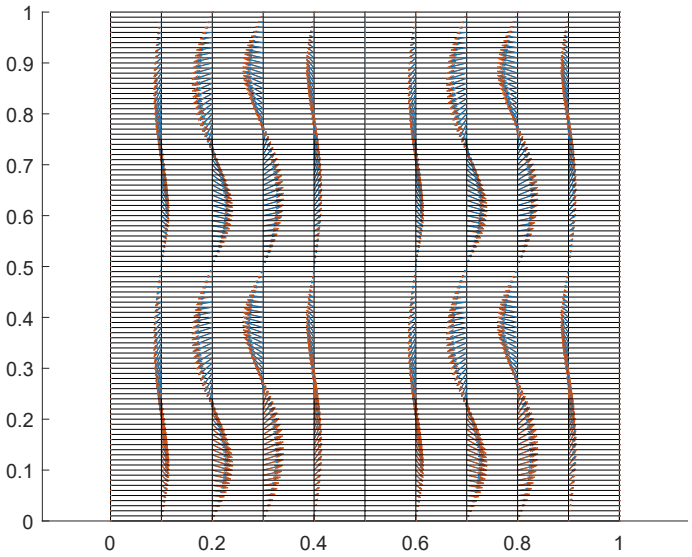

Figure 5.7: Rectangles velocity field

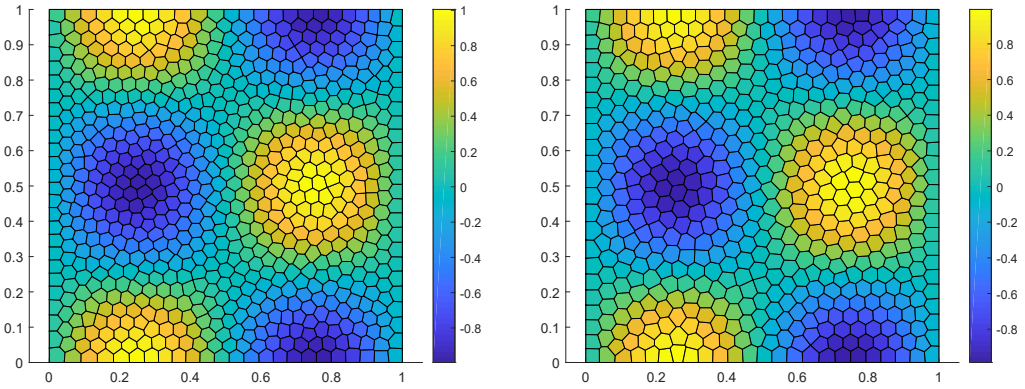

(a) 750 elements

(b) 600 elements

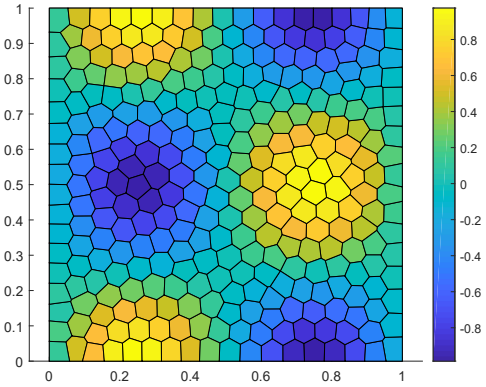

(c) 300 elements

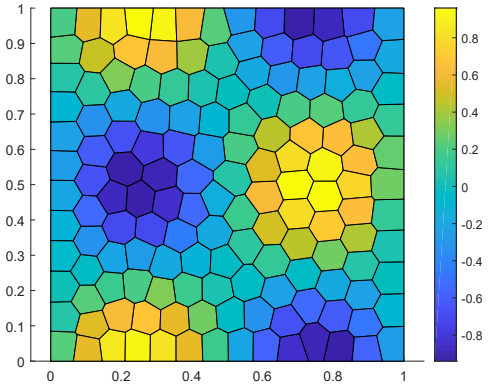

(d) 150 Elements

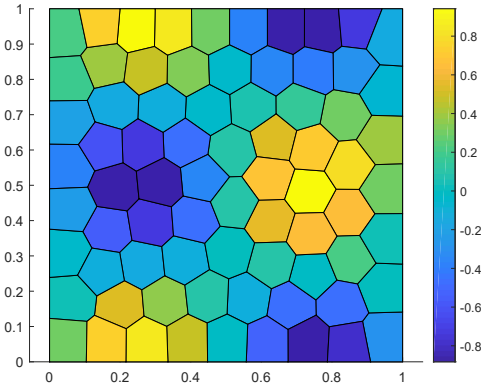

(e) 75 Elements

Figure 5.8: Voronoi meshes pressure field

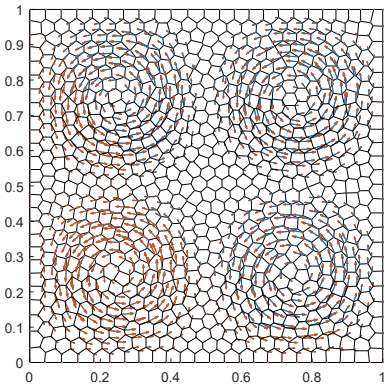

(a) 750 elements

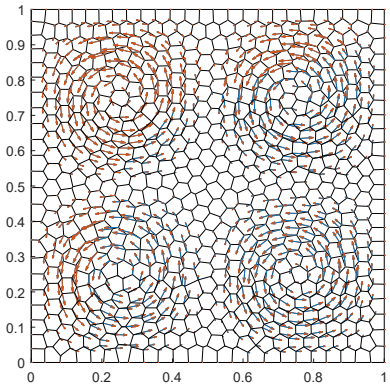

(b) 600 elements

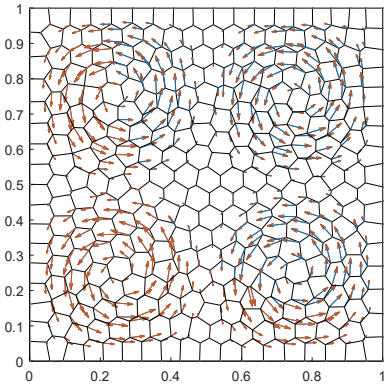

(c) 300 elements

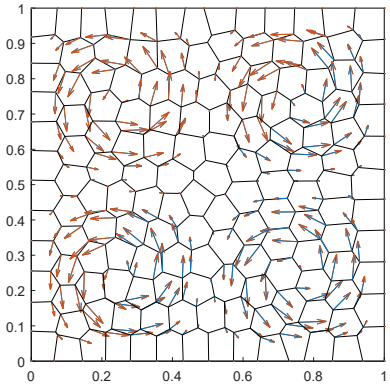

(d) 150 Elements

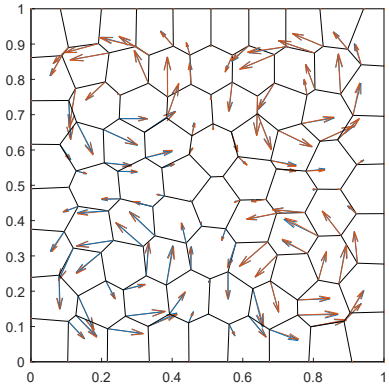

(e) 75 Elements

Figure 5.9: Voronoi meshes velocity field

In addition to a simple domain such as the square, it was decided to test a case with a slightly more complex domain. Therefore, the following mesh has been created using PolyMesher within a domain with a rounded shape and two holes.

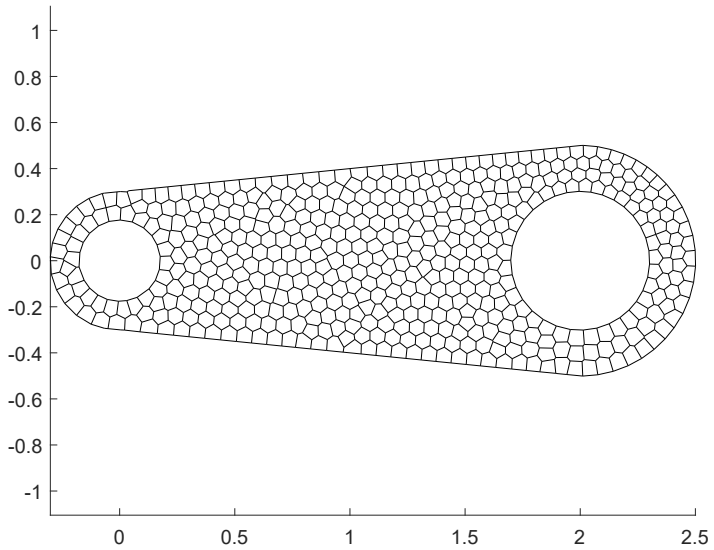

Figure 5.10: Wrench mesh

The boundary conditions have been set as follows:

- Dirichlet homogeneous condition at the outer edge of the domain
- Neumann homogeneous condition in the degrees of freedom at the holes.

A unitary force along the x-axis direction has been applied to some degrees of freedom. Having defined the problem in this way, we expect that a direct flow will be generated from one the left hole to the right one.

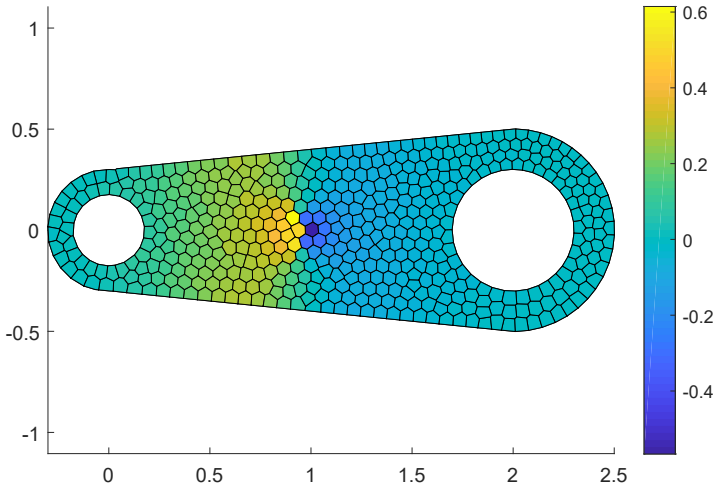

Figure 5.11: Wrench pressure field

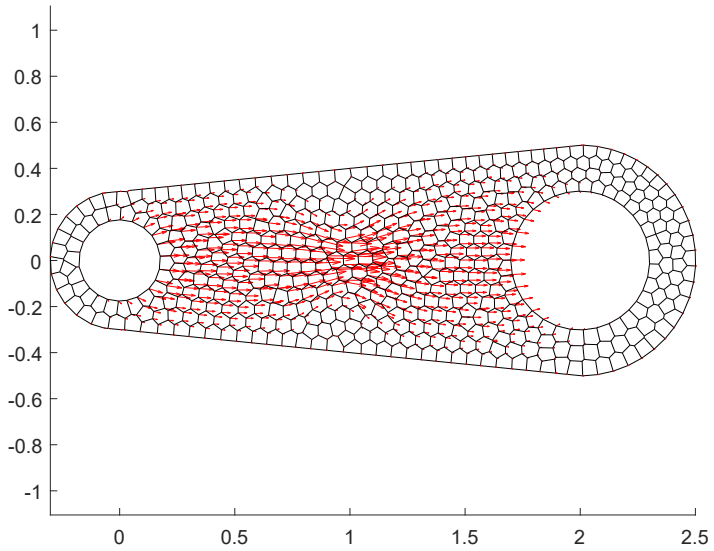

Figure 5.12: Wrench velocity field

5.0.1 Error evaluation

The expected rate of convergence for the errors, according to [6], is:

$$\|\mathbf{u} - \mathbf{u}_h\|_{L^2(\Omega)} \leq h^{k+1}|\mathbf{u}|_{k+1} + h^{k+3}|\mathbf{f}|_{k+1} \tag{5.3}$$

$$\|p - p_h\|_{L^2(\Omega)} \leq h^{k}|\mathbf{u}|_{k+1} + h^{k}|p|_{k} + h^{k+2}|\mathbf{f}|_{k+1} \tag{5.4}$$

where $(\mathbf{u}_h, p_h)$ represent the discrete solution of the Problem 2.1 and $(\mathbf{u}, p)$ represent the continuous solution (5.1) and (5.2).

$$\text{error}(\mathbf{u}, L^2) \coloneqq \frac{1}{\|\mathbf{u}\|_{L^2(\Omega)}} \sqrt{\sum_{E \in \Omega_h} \|\mathbf{u} - \Pi_k^0 \mathbf{u}_h\|^2_{L^2(E)}} \tag{5.5}$$

$$\text{error}(p, L^2) \coloneqq \frac{1}{\|p\|_{L^2(\Omega)}} \|p - p_h\|_{L^2(\Omega)} \tag{5.6}$$

To evaluate the L^2 norm, the following integrals must be solved:

$$\|\mathbf{u}\|_{L^2(\Omega)} = \sqrt{\int_\Omega |\mathbf{u}|^2 \, d\Omega} = \sqrt{\sum_{E \in \mathcal{T}_h} \int_E |u_x|^2 + |u_y|^2 \, dE} \tag{5.7}$$

$$\|\mathbf{u} - \Pi_k^0 \mathbf{u}_h\|^2_{L^2(E)} = \int_E |u_x - \Pi_k^0 u_{h,x}|^2 + |u_y - \Pi_k^0 u_{h,y}|^2 \, dE \tag{5.8}$$

$$\|p\|_{L^2(\Omega)} = \sqrt{\int_\Omega |p|^2 \, d\Omega} = \sqrt{\sum_{E \in \mathcal{T}_h} \int_E |p|^2 \, dE} \tag{5.9}$$

$$\|p - p_h\|_{L^2(\Omega)} = \sqrt{\int_\Omega |p - p_h|^2 \, d\Omega} = \sqrt{\sum_{E \in \mathcal{T}_h} \int_E |p - p_h|^2 \, dE} \tag{5.10}$$

We have chosen to use Gauss quadrature formulas to integrate the squared function element by element. As for the function $\mathbf{u}_h$, this is defined only in the degrees of freedom, and it is necessary to compare the exact solution with a polynomial projection of the discrete solution. Then, the Π_k^∇ projection has been used to obtain a polynomial function. By doing so, both the exact and the approximate functions have been evaluated in the Gauss quadrature nodes.

The pressure p_h is already defined as a polynomial inside each element and it is sufficient to multiply the Vandermonde matrix by the solution p_h to obtain the values of p_h in the quadrature nodes.

As shown in these figures, the order of convergence follows the theoretical trend.

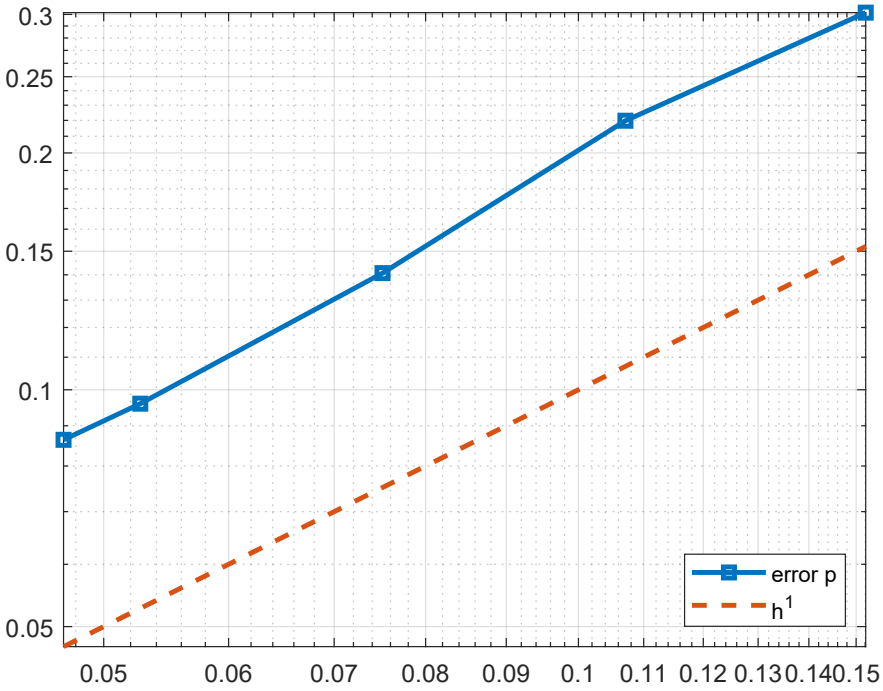

Figure 5.13: L^2 error pressure, k=1

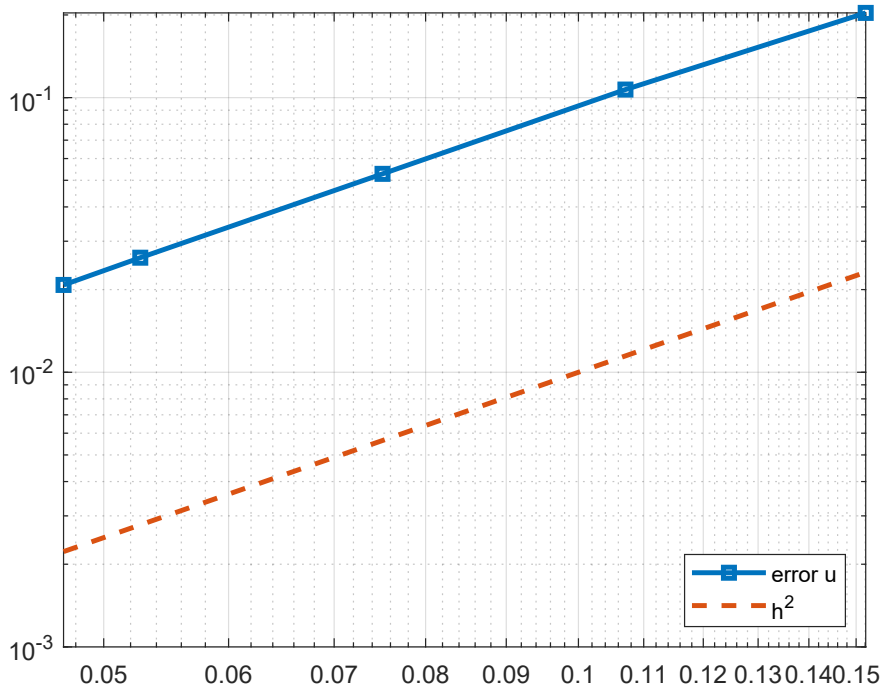

Figure 5.14: L^2 error velocity, k=1

Chapter 6

Conclusions and future developments

In this thesis the Stokes problem has been analysed through the employment of the virtual element method. The variational formulation of this problem was derived, along with the structure of the virtual elements needed to solve this kind of partial differential equation. The main challenges were posed by the fact that the Stokes equation solves two coupled fields: the velocity one (which is a vector) and the pressure one. This increases both the formulation difficulty and the computational complexity with respect to simpler problems, such as the deformation of an elastic plate.

Matlab was used to implement the virtual element method of order one and two; also, a reduced formulation was analysed, which allowed to lessen the number of degrees of freedom, and thus the computational complexity, while maintaining unchanged the results. For each case, the functional spaces and the associated degrees of freedom were analysed and the L^2 and H^1 projectors were implemented. To do this, it was necessary to choose suitable polynomial basis for each space considered.

The Stokes problem was solved on different meshes of a simple two-dimensional square domain; the main advantage of VEM is the much greater flexibility in the choice of mesh elements with respect to traditional finite element methods. Namely, elements with very large aspect ratios and varying shapes can be used in VEMs.

Furthermore, this VEM approach to the solution of the Stokes problem generates a discrete velocity field which is pointwise divergence-free, while the finite elements method do not allow to obtain a truly vanishing divergence. Therefore, the proposed method is worthy of attention even for the solution of the Stokes problem on triangular or square meshes.

In all cases, the VEM formulation produced results which were in very good agreement with the exact solution, which is known for this particular problem. The error convergence rate was also calculated exploiting a series of regular meshes, one

more refined than the other. In the first order formulations both the pressure and the velocity converged at the expected rate, which is, respectively, 1 and 2.

Future developments of the presented work may include:

- The definition of an automated procedure to define elements of any order.
- A rewriting of the main routines of the numerical code, with a focus on computational performance.
- The application of the virtual element method to different problems and more complex geometries.

Bibliography

[1] L Beirão da Veiga et al. "Basic principles of virtual element methods". In: *Mathematical Models and Methods in Applied Sciences* 23.01 (2013), pp. 199–214.

[2] L Beirão da Veiga et al. "The hitchhiker's guide to the virtual element method". In: *Mathematical models and methods in applied sciences* 24.08 (2014), pp. 1541–1573.

[3] L Beirão da Veiga et al. "Virtual element method for general second-order elliptic problems on polygonal meshes". In: *Mathematical Models and Methods in Applied Sciences* 26.04 (2016), pp. 729–750.

[4] S. Berrone and A. Borio. "An optimized implementation of the Virtual Element Method for second order PDEs". 2020.

[5] A. Borio. *VEM implementation example*. 2020. URL: `https://github.com/andrea-borio/vem-implementation-example`.

[6] Franco Dassi and Giuseppe Vacca. "Bricks for the mixed high-order virtual element method: Projectors and differential operators". In: *Applied Numerical Mathematics* 155 (2020), pp. 140–159.

[7] Lourenco Beirão da Veiga, Carlo Lovadina, and Giuseppe Vacca. "Divergence free virtual elements for the Stokes problem on polygonal meshes". In: *ESAIM: Mathematical Modelling and Numerical Analysis* 51.2 (2017), pp. 509–535.

[8] Glaucio H. Paulino. *PolyMesher*. 2012. URL: `https://paulino.ce.gatech.edu/software.html`.

[9] Alfio Quarteroni. *Modellistica numerica per problemi differenziali*. Vol. 97. Springer, 2016.